

PYL8 mediates ABA perception in the root through non-cell-autonomous and ligand stabilization based mechanisms

Borja Belda-Palazon¹, Mary-Paz Gonzalez-Garcia², Jorge Lozano-Juste¹, Alberto Coego¹, Regina Antoni¹, Jose Julian¹, Marta Peirats-Llobet¹, Lesia Rodriguez¹, Ana Berbel¹, Daniela Dietrich³, Maria A. Fernandez¹, Francisco Madueño¹, Malcolm J. Bennett³, and Pedro L. Rodriguez*¹

¹Instituto de Biología Molecular y Celular de Plantas, Consejo Superior de Investigaciones Científicas-Universidad Politécnica de Valencia, ES-46022 Valencia, Spain.

²Centro Nacional de Biotecnología-CSIC, Cantoblanco, E-28049 Madrid, Spain

³Centre for Plant Integrative Biology, School of Biosciences, University of Nottingham, LE12 5RD, UK

*Address correspondence to Pedro L. Rodriguez prodriguez@ibmcp.upv.es
Instituto de Biología Molecular y Celular de Plantas (CSIC-UPV)
Avd de los Naranjos s/n. Edificio CPI, 8E. Valencia 46022. Spain
Phone: +34 963877860

Abstract

The phytohormone abscisic acid (ABA) plays a key role regulating root growth, root system architecture and root adaptive responses, such as hydrotropism. The molecular and cellular mechanisms that regulate the action of core ABA signaling components in roots are not fully understood. ABA is perceived through receptors from the PYR/PYL/RCAR family and PP2C co-receptors. PYL8/RCAR3 plays a non-redundant role in regulating primary and lateral root growth. Here we demonstrate that ABA specifically stabilizes PYL8 compared to other ABA receptors and induces accumulation of PYL8 in root nuclei. This requires ABA perception by PYL8 and leads to diminished ubiquitination of PYL8 in roots. The ABA agonist quinabactin, which promotes root ABA signaling through dimeric receptors, fails to stabilize the monomeric receptor PYL8. Moreover, a PYL8 mutant unable to bind ABA and inhibit PP2C is not stabilized by the ligand, whereas a PYL8^{5KR} mutant is more stable than PYL8 at endogenous ABA concentrations. The PYL8 transcript was detected in the epidermis and stele of the root meristem; however the PYL8 protein was also detected in adjacent tissues. Expression of PYL8 driven by tissue-specific promoters revealed movement to adjacent tissues. Hence both inter- and intracellular trafficking of PYL8 appears to occur in the root apical meristem. Our findings reveal a novel non-cell-autonomous mechanism for hormone receptors and help explain the non-redundant role of PYL8 mediated root ABA signaling.

Significance statement

The phytohormone abscisic acid (ABA) controls root responses to environmental signals such as abiotic stress. ABA signaling in roots depends on the non-redundant role of the PYL8 receptor. This study reveals special features of this ABA receptor. ABA binding triggers hormone-dependent stabilization of PYL8 through reduced ubiquitination and induces nuclear localization of the receptor. ABA-induced stabilization also allows movement of the PYL8 receptor from the root epidermis and stele to adjacent tissues. Hence, like mobile transcription factors that regulate plant development, the PYL8

protein can move between cells. In summary, our study reports a novel non-cell-autonomous mechanism to regulate hormone perception and root growth.

\body

Introduction

Responses to environmental conditions in plant roots are coordinated by different hormones. Thus, hormone signaling regulates root growth, root system architecture and tropic root responses (1-3). Abscisic acid (ABA) mediates root responses to different environmental factors, such as the presence of nitrate in the soil, water deficit, moisture gradients, salt or nutrient deficiency (4). ABA signaling through the PYRABACTIN RESISTANCE1 (PYR1)/PYR1-LIKE (PYL)/REGULATORY COMPONENTS OF ABA RECEPTORS (RCAR)- Protein phosphatases type 2C (PP2Cs) and ABA-activated SNF1-related protein kinases (SnRK2s) core components is linked to different plant adaptive responses to water deficit and osmotic and salt stress, such as the maintenance of primary root elongation and the repression of lateral root formation (4-10). For instance, in maize seedlings under water-deficit stress the primary root growth is maintained through ABA action, which acts partially through ethylene antagonism (5). In Arabidopsis roots exposed to salt stress, ABA also has a growth-promoting role during the recovery phase (11). Additionally, ABA signaling is required for root hydrotropism, an adaptive response that facilitates soil exploration under heterogeneous water availability (3). Regulation of root growth by ABA is closely connected with hydrotropism, as the hydrotropic response involves asymmetric ABA signaling in the root cortex through the PYR/PYL/RCAR-PP2C-SnRK2 core signaling pathway (3, 12, 13). Other environmental cues, such as salinity, induce root adaptations that are mediated by ABA (10, 14, 15). Nutrient-induced root plasticity is also regulated by ABA, for example the suberization of the endodermis in response to either sodium chloride treatment or sulfur or potassium deficiencies (14). Thus, harmful minerals can be excluded by the endodermis.

Although the role of ABA in root physiology has been well studied, the molecular and cellular mechanisms that operate to coordinate the action of core components are not well known. For instance, the expression of the ABA-

activated kinase SnRK2.2 is observed in all root tissues, but expression of the ABA receptor promoters is restricted to some of them (3, 13). Therefore, it is not well known how ABA perception is connected with the activation of SnRK2.2 in different root tissues. Additionally, different PYR/PYL/RCAR ABA receptors are expressed at high levels and contribute to the quantitative regulation of ABA sensitivity in the root, but uniquely the *pyl8/rcar3* single knockout shows reduced sensitivity to ABA-mediated inhibition of root growth (8, 13). Therefore, PYL8/RCAR3 plays a non-redundant role for ABA signaling in the root, which relies on PYL8-mediated inhibition of at least five clade A protein phosphatases type 2C (PP2Cs), i.e. HAB1, HAB2, ABI1, ABI2 and PP2CA (13). Compared to other ABA receptors, PYL8 shows a unique expression pattern in the root epidermis and lateral root cap (13). Recent studies investigating the degradation of ABA receptors in seedlings have revealed that PYL8 is ubiquitinated and degraded by the 26S proteasome in *Arabidopsis thaliana* (16, 17). In those studies, we found that ABA treatment increased PYL8 protein levels, but had no significant effect on other receptors such as PYR1 and PYL4 (17). Moreover, ABA treatment limited PYL8 degradation in seedlings and reduced PYL8 polyubiquitination (16). It is currently unknown whether such a mechanism operates in root tissues or whether ligand perception by either PYL8 or other receptors is required to stabilize PYL8. Further investigation of ligand-induced effects on PYL8 stability might help explain its non-redundant role for ABA signaling in roots.

Studies to investigate how different hormones control root growth, tropic root responses or stress adaptation have revealed single tissue layers or discrete spatial domains that are differentially targeted by hormones (1). For instance, auxin targets elongating epidermal cells during the gravitropic response whereas ABA targets elongating cortical cells during the hydrotropic response (3, 18). On the other hand, endodermal ABA signaling promotes lateral root quiescence under saline conditions (9). ABA also promotes quiescence of the quiescent center (QC), which may be considered as positive regulation of root growth as it promotes QC maintenance (19). However, ABA also inhibits cell division in the proximal part of *Arabidopsis* root meristem, which can explain the inhibitory effect of high ABA concentrations on root growth (19). In contrast, low levels of ABA promote root elongation through

increased rate of cell production and elongation (3). ABA signaling is also important in the mature root, where most of the absorption of minerals and water takes place (8). In agreement with the above mentioned physiological studies, the expression pattern of SnRK2.2 indicates that ABA signaling is required in all root tissues (3). Altogether these studies suggest that ABA perception in different root domains is important to regulate root physiology and root growth; however, a detailed molecular and cellular understanding of root ABA perception is still lacking in the different root tissues where ABA acts.

Results

ABA specifically stabilizes the PYL8 receptor

ABA receptor stability and degradation is an emerging topic in ABA signaling (16, 17, 20, 21). In order to obtain a comprehensive picture of the turnover of ABA receptors, we analyzed protein dynamics of ten epitope (HA)-tagged receptors (PYR1, PYL1, PYL2, PYL4, PYL5, PYL6, PYL7, PYL8, PYL9 and PYL10, the most highly expressed gene products of the gene family) in 2-week-old plants. Treatment with the translation inhibitor cycloheximide (CHX) led to diminished protein synthesis of all ABA receptors, whereas treatment with the proteasome inhibitor MG132 led to their accumulation (Fig. 1A). Interestingly, addition of ABA specifically led to the accumulation of PYL8 protein (Fig. 1A). ABA treatment of transgenic lines that express GFP-tagged versions of PYL2, PYL4, and PYL8 also revealed a selective ABA-induced accumulation of PYL8 (Fig. 1B and C). qRT-PCR analyses corroborated that this effect was not caused by changes in the expression of 35S promoter-driven 3HA- or GFP-tagged transgenes (SI Appendix, Fig. S1). ABA therefore appears to enhance PYL8 accumulation in these lines through a post-transcriptional mechanism. Confocal laser scanning microscopy (CLSM) also revealed that GFP-PYL8 exhibited a predominantly nuclear localization in root cells following ABA treatment, whereas GFP-PYL2 and GFP-PYL4 localized to both the nucleus and cytosol of mock or ABA-treated roots (Fig. 1C).

To gain insight on the root localization of PYL8, we expressed PYL8-GFP driven by its own promoter in a *pyl8-1* mutant background (*ProPYL8:PYL8-GFP pyl8-1*). PYL8-GFP complemented the ABA-insensitive *pyl8-1* phenotype in a

root growth assay, indicating that PYL8-GFP is functional (Fig. 2A). Next, we analyzed PYL8-GFP protein levels in roots by immunoblotting and found that it was increased 5-7 fold after ABA treatment (Fig. 2B). qRT-PCR analysis showed that ABA treatment does not induce upregulation of the *PYL8* transcript; in fact ABA down-regulates *PYL8* gene expression (Fig. 2B), in agreement with previous reports in seedlings (22, 23). Instead, ABA treatment led to an accumulation of PYL8-GFP in the nucleus; as observed for GFP-PYL8 expressed from a 35S promoter (Fig. 1C and 2C). Next, we investigated whether PYL8-GFP fluorescence may report changes in ABA concentration in the root. A dose-response analysis indicated that PYL8-GFP fluorescence was sensitive to changes in ABA concentration induced by exogenous ABA addition or osmotic stress (Fig. 2D-E; SI Appendix, Fig. S2A-B). Finally, a kinetic analysis of PYL8-GFP fluorescence was performed in response to 10 μ M ABA treatment and a gradual increase of the fluorescent signal, which could be detected from 30 min after ABA treatment, was observed (SI Appendix, Fig. S2C). We conclude that ABA specifically stabilizes the PYL8 receptor and leads to its accumulation in root cell nuclei.

PYL8 stabilization in roots is triggered by ligand binding and requires PP2C interaction

In order to investigate whether the enhanced PYL8-GFP fluorescence observed after ABA treatment requires ligand perception by PYL8 or simply reflects hormone signaling through other ABA receptors that also operate in the root (13), we switched on ABA signaling through quinabactin (QB) treatment. QB is an ABA agonist that does not activate the PYL8 receptor (SI Appendix, Fig. S3A) instead activating ABA signaling primarily through dimeric ABA receptors such as PYR1, PYL1 and PYL2, which are expressed at high level in the root and contribute to the quantitative regulation of ABA signaling (13, 24, 25). QB treatment was able to upregulate the expression of the ABA-responsive ProRAB18:GFP reporter, but in contrast to ABA, QB did not enhance PYL8-GFP fluorescence (Fig. 3A). Therefore, the PYL8-GFP accumulation appears to require ABA perception by PYL8.

To ascertain whether ABA treatment leads to decreased degradation of PYL8 in roots, we performed a CHX \pm ABA experiment using the

ProPYL8:PYL8-GFP pyl8-1 line and analyzed PYL8 protein levels in roots (Fig. 3B). Whilst CHX treatment in the absence of ABA led to a 60% reduction of PYL8 after 120 min, the simultaneous presence of ABA slowed PYL8 degradation to a reduction of only 20%. QB was not effective in slowing PYL8 degradation (Fig. 3B). ABA may prevent degradation of PYL8 in roots through reduced polyubiquitination of the receptor (16). To investigate this possibility, we performed immunoprecipitation of HA-PYL8 in mock and ABA-treated root samples. Immunoprecipitated HA-PYL8 was analyzed using anti-HA and anti-Ub (P4D1) antibodies and the ratio of Ub(n)-PYL8 to PYL8 was found to be approximately 6-fold higher in mock compared to ABA-treated roots (Fig. 3C). Thus, even though the total PYL8 protein level was increased about 4-fold after ABA treatment, the amount of polyubiquitinated PYL8 was diminished in ABA-treated roots compared to mock conditions (Fig. 3C). In contrast, ABA treatment did not affect the ubiquitination ratio of PYL2 and PYL9 compared to mock conditions (Fig. 3C).

The results described above using QB treatment suggest that PYL8 stabilization and/or accumulation requires ABA perception by the receptor. In order to obtain further evidence we analyzed the PYL8^{K61R Y120A} mutant, which is predicted to be unable to bind ABA because it is impaired both in the salt bridge formed between the highly conserved K61 residue and the carboxylate of ABA, and the hydrogen bond formed by Y120 with the ABA carboxylate group through an internal water molecule (13). Accordingly, recombinant PYL8^{K61R Y120A} protein was unable to inhibit PP2C HAB1 (Figure 3D). We generated GFP-PYL8^{K61R Y120A} transgenic lines and analyzed them following ABA treatment (Fig. 3E). Both CLSM and immunoblot analysis of root protein extracts revealed that GFP-PYL8^{K61R Y120A} fails to accumulate after ABA treatment, in contrast to wild-type PYL8 (Figure 3E). We conclude that either ABA perception and/or PP2C interaction are required to trigger PYL8 stabilization. Recent proteomic studies led to the identification of ubiquitinated residues in PYL8 (26). In contrast to the K61 residue that affects ABA binding, other N-terminal Lys residues of PYL8 are not predicted to be involved in ABA binding (26). We therefore decided to mutate those Lys residues which are potential ubiquitination sites (26) but presumably do not impair PYL8 function, i.e. Lys24, Lys38, Lys59, Lys70 and Lys84, and generated the quintuple Lys-Arg PYL8

mutant (abbreviated as 5KR). We found that in vitro activity of the 5KR mutant was comparable to wild-type PYL8 (Fig. 3D). Interestingly, GFP- and HA-tagged lines of PYL8^{5KR} showed a 2-3 fold increase of protein levels compared to wild type in the absence of exogenous ABA treatment (Fig. 3E; SI Appendix, Fig. S3B). We analyzed seedling establishment in the presence of 0.5 μ M ABA and ABA-mediated inhibition of root growth in response to 10 μ M ABA (SI Appendix, Fig. S3C-D). In both cases, HA-tagged lines of PYL8^{5KR} showed enhanced sensitivity to ABA compared to lines expressing wild-type PYL8. These results suggest that ubiquitination and regulation of PYL8 protein stability is crucial for proper response to ABA.

In order to investigate whether intracellular movement of PYL8 affects plant sensitivity to ABA, we have compared sub-cellular localization and ABA sensitivity of GFP-PYL8, GFP-PYL8^{5KR} and GFP-PYL8^{K61R Y120A} lines (SI Appendix, Fig. S4). The line expressing GFP-PYL8, which accumulates GFP-PYL8 in the nucleus after ABA-treatment, shows enhanced sensitivity in ABA-mediated inhibition of root growth and repression of lateral root formation compared to wild-type Col-0 (SI Appendix, Fig. S4). Some nuclear accumulation of GFP-PYL8^{5KR} was observed at endogenous ABA levels (SI Appendix, Fig. S4A), which correlated with enhanced sensitivity to ABA compared to GFP-PYL8 line (SI Appendix, Fig. S4B-C; see also Fig. S3C-D). In contrast, lines expressing GFP-PYL8^{K61R Y120A}, which does not accumulate in nucleus after ABA treatment, behave as wild-type Col-0 in root growth assays (SI Appendix, Fig. S4). Therefore, nuclear accumulation of GFP-PYL8 induced by ABA is required for ABA response.

PYL8 behaves non-cell-autonomously in root tissues

In order to study the effect of ABA treatment on PYL8 expression in the root apex, we performed GUS staining after mock or 50 μ M ABA treatment for 3h (Fig. 4A). In control root apices, GUS expression driven by the PYL8 promoter was detected in lateral root cap (LRC), root epidermis and stele cells (SI Appendix, Fig. S5A-B), as previously reported (13). This PYL8 expression pattern was similar in ABA-treated plants, although some attenuation of PYL8 expression was apparent (Fig. 4A). To gain further insight about the expression

of *PYL8* in the root apex, we performed in situ hybridization using a digoxigenin-labeled antisense RNA probe to detect the *PYL8* mRNA in Col-0 (Fig. 4B). Under both mock and ABA-treatment conditions the *PYL8* transcript was mainly detected in the epidermis. Weak staining of stele cells using the antisense RNA probe was also detected, but was attenuated after ABA treatment (Fig. 4B).

Since ABA signaling has been reported to regulate distinct processes in different root tissues (3, 9, 19) and *PYL8* plays a key role in root ABA perception, we investigated the localization of the *PYL8* protein in the root apex. Using CLSM we analyzed the Pro*PYL8*:*PYL8*-GFP lines either after mock or ABA treatments. Interestingly, expression of *PYL8*-GFP in mock-treated roots was weakly detected in the epidermis and stele, whereas following ABA-treatment it was clearly visible in LRC, epidermis, cortex, endodermis, stele, quiescent center and columella cells (Fig. 4C). *PYL8*-GFP expression in the epidermis was markedly enhanced by ABA treatment (SI Appendix, Movie S1). Since the *PYL8* transcript was not detected in the cortex or endodermis, we conclude that the *PYL8* protein is translocated to adjacent tissues from cells where it is initially synthesized. This movement is reminiscent of mobile transcription factors (TFs) such as *SHORT ROOT* (*SHR*) that regulate root development (27). To further investigate the movement of *PYL8* between different root layers, we expressed *PYL8*-GFP driven by *WER* and *WOL* tissue-specific promoters (3) (SI Appendix), and examined the localization of the fluorescent protein by CLSM (Fig. 4D-E). Quantification of CLSM images was performed with an updated version of CellSeT software (Fig. 4D-E), which performs tissue-scale measurements from confocal microscope images (SI Appendix). When *PYL8*-GFP was expressed under control of the *WER* promoter, which drives expression in epidermis and LRC (as confirmed by a *pWER:GFP* control), we could also detect *PYL8*-GFP at least in cortex cells (Fig. 4D). In the case of *WOL*-driven expression, whereas the GFP control was detected in the root vascular cylinder and pericycle as expected, we could detect *PYL8*-GFP additionally in the lateral root cap, epidermis, cortex and endodermis (Fig. 4E). Taken together, these results suggest that the *PYL8* protein can move from the cells where its transcript is produced.

The ABA-insensitive phenotype of *pyl8-2* in root growth assays was not complemented when *PYL8* was expressed driven by either *WER* or *WOL* promoters (SI Appendix, Fig. S6). *PYL8* mRNA expression driven by its endogenous promoter is mostly localized in LRC, epidermis and the vascular bundle, and is able to complement the ABA insensitivity of *pyl8* in root growth assays (Fig. 2A). Driven by *WER* promoter *PYL8* protein was markedly detected in lateral root cap and epidermis, and weakly in cortex, suggesting that complementation requires intercellular movement of the protein to other root layers. Driven by *WOL* promoter *PYL8* protein was detected in most of root tissues; however expression levels were markedly lower than those obtained using the endogenous *PYL8* promoter (Fig. 4E and 4C). Therefore, although intercellular movement of the protein seems to be necessary, it is not sufficient unless suitable levels of the protein are achieved. Taken together, these results suggest that combined expression in epidermis and vascular bundle is required for complementation of the *pyl8* phenotype (Fig. 2A).

Finally, given the importance of ABA signaling in the mature root, expression of *PYL8*-GFP was examined in the root differentiation zone after ABA treatment and was localized in the epidermis, cortex, endodermis, pericycle, and vascular tissue (SI Appendix, Fig. S5C-D). In particular, a 3D reconstruction after CSLM imaging revealed the presence of *PYL8* in procambial cells of the vascular tissue (SI Appendix, Movie S2), which suggests a possible role of *PYL8* in vascular development.

Discussion

We report that, unlike other ABA receptors, *PYL8* exhibits distinct regulatory properties. For example, *PYL8* is transcribed in the epidermis and stele of the root apex but the *PYL8* protein is also present in the cortex and endodermis. Hence, comparison of the *PYL8* transcript expression with the localization of the *PYL8* protein reveals translocation of the ABA receptor from epidermis or stele to adjacent tissues, including the cortex and endodermis (Figure 5A). Moreover, when *PYL8*-GFP was expressed driven by the *WOL* promoter, which is specifically expressed in the root vascular cylinder, the protein moved as far as the lateral root cap (Figure 4E). Hence, *PYL8* appears to regulate ABA signaling in the root apex through a non-cell autonomous mechanism. **However, it seems**

that both intercellular movement and appropriated protein levels are required for complementation of the ABA-insensitive phenotype of *pyl8* in root growth assays (Fig. 4C and Fig. 2A). The regulatory behaviour exhibited by PYL8 is reminiscent of mobile TFs involved in plant development that perform non-cell-autonomous actions by trafficking from cell to cell through plasmodesmata (28, 29). For instance, SHORT ROOT (SHR) which is synthesized in all stele cells except the phloem, moves to adjacent cells including the endodermis and phloem (28, 29). The movement of SHR relies on the endomembrane system, interaction with the SHR interacting embryonic lethal (SIEL) protein and association to endosomes in a SIEL-dependent manner (27). Interestingly, ABA receptors traffic through endosomes (20, 21). In addition to degradation in the vacuole, endosome trafficking can promote signaling functions both in plants and animals by facilitating the movement of proteins between cells (30).

We also report that ABA specifically stabilizes PYL8 compared to other ABA receptors and induces its accumulation in root nuclei. We demonstrate that this requires ABA perception by PYL8 and leads to diminished ubiquitination of PYL8 in roots. Thus, the inactive PYL8^{K61R Y120A} protein is not stabilized by ABA in roots, and activation of root ABA signaling in the absence of ligand binding by PYL8 (as occurs after QB treatment) fails to stabilize PYL8. Different reporters for direct visualization of ABA concentration changes have been described (31-34). However, reporters based on the overexpression of PP2Cs or ABA receptors affect ABA sensitivity per se, for instance ABAleon lines show reduced sensitivity to ABA (33) whereas ABACUS lines show enhanced ABA-mediated inhibition of root growth compared to wild type (34). The ProPYL8:PYL8-GFP *pyl8-1* line here described showed wild-type sensitivity to ABA-mediated inhibition of root growth (Fig. 2A), which is a requisite for a root ABA biosensor. Additionally both kinetic and dose-response analyses indicate that PYL8-GFP might be used as an ABA biosensor in roots to detect exogenous ABA (SI Appendix, Fig. S2). Moreover, the PYL8-GFP biosensor harbors the potential to specifically identify PYL8 agonists through *in vivo* screening, which is required to confirm the bioactivity of molecules identified by *in vitro* or *in silico* screening. However, the current version of the PYL8-GFP biosensor needs to be improved to a ratiometric version in order to achieve a wider dynamic range of sensitivity to ABA changes (33, 34).

Although the main function of PYL8 is the ABA-dependent inhibition of clade A PP2Cs such as ABI1 and PP2CA (13), an additional role independent of the core ABA signaling pathway has also been reported (35). Thus, PYL8 promotes lateral root growth by interacting with the TFs MYB77, MYB44 and MYB73 to augment auxin signaling, which points to an additional nuclear role of PYL8 (35). ABA perception by PYL8 in the nucleus is required to inhibit PP2C activity and hence relieve repression of ABA signaling by the SWI/SNF chromatin remodeling ATPase BRAHMA (36). Failure to inhibit nuclear PP2C activity, as exemplified by the phosphatase *abi1*^{Gly180Asp} that is refractory to inhibition by ABA receptors, blocks ABA signaling and inhibits ABA response element-binding bZIPs that mediate transcriptional response to ABA (37, 38). Interestingly, we observed enhanced nuclear localization of PYL8 in root cells after ABA treatment, which suggests that both intra- and inter-cellular movement of PYL8 occurs (Figure 5B). Further insight into the cellular mechanisms involved in movement of ABA receptors is a key issue for future research. We note that the enhanced localization of PYL8 in the nucleus together with diminished polyubiquitination induced by ABA can reduce degradation of the receptor through the vacuolar pathway (20, 21) and contributes to stabilization of the receptor (Figure 5B). The mechanism whereby ABA specifically reduces polyubiquitination of PYL8 is another challenging issue to be investigated.

Materials and Methods

Detailed description is provided in SI Appendix for plant material and growth conditions, generation of HA-tagged and GFP-tagged lines and ProPYL8:PYL8-GFP *pyl8-1* lines, expression of PYL8-GFP in root driven by tissue-specific promoters, generation of PYL8 mutations, *in vivo* protein analysis and degradation assays, root growth assays, RT-qPCR analysis, GUS staining, PP2C inhibition assays, RNA in situ hybridization, Confocal Laser Scanning Microscopy (CLSM), measurements and statistical analysis.

Acknowledgements

Work in the Rodriguez and Madueño laboratories was supported by the Ministerio de Ciencia e Innovacion, Fondo Europeo de Desarrollo Regional and

Consejo Superior de Investigaciones Científicas (grants BIO2014-52537-R and BIO2017-82503-R to P.L.R. and BIO2015-64307-R to F.M.). J.L.-J. was supported by a Juan de la Cierva contract from MINECO and by the Marie Skłodowska-Curie Action H2020-MSCA-IF-2015-707477. B.B. was funded by Programa VALi+d GVA APOSTD/2017/039. J.J. was supported by a FPI contract from MINECO and M.A.F by a FPU contract from MINECO. D.D and M.J.B were supported by the BBSRC [grant number BB/M002136/1] and Leverhulme Trust [grant number RPG-2016-409].

References

1. Ubeda-Tomas S, Beemster GT, & Bennett MJ (2012) Hormonal regulation of root growth: integrating local activities into global behaviour. *Trends Plant Sci* 17(6):326-331.
2. Bao Y, *et al.* (2014) Plant roots use a patterning mechanism to position lateral root branches toward available water. *Proc Natl Acad Sci USA* 111(25):9319-9324.
3. Dietrich D, *et al.* (2017) Root hydrotropism is controlled via a cortex-specific growth mechanism. *Nature Plants* 3:17057.
4. Harris JM (2015) Abscisic Acid: Hidden Architect of Root System Structure. *Plants* 4(3):548-572.
5. Spollen WG, LeNoble ME, Samuels TD, Bernstein N, & Sharp RE (2000) Abscisic acid accumulation maintains maize primary root elongation at low water potentials by restricting ethylene production. *Plant Physiol* 122(3):967-976.
6. Sharp RE, *et al.* (2004) Root growth maintenance during water deficits: physiology to functional genomics. *Journal Exp Bot* 55(407):2343-2351.
7. Deak KI & Malamy J (2005) Osmotic regulation of root system architecture. *The Plant Journal* 43(1):17-28.
8. Gonzalez-Guzman M, *et al.* (2012) Arabidopsis PYR/PYL/RCAR receptors play a major role in quantitative regulation of stomatal aperture and transcriptional response to abscisic acid. *The Plant Cell* 24(6):2483-2496.
9. Duan L, *et al.* (2013) Endodermal ABA signaling promotes lateral root quiescence during salt stress in Arabidopsis seedlings. *The Plant Cell* 25(1):324-341.
10. Feng W, Lindner H, Robbins NE, 2nd, & Dinneny JR (2016) Growing Out of Stress: The Role of Cell- and Organ-Scale Growth Control in Plant Water-Stress Responses. *The Plant Cell* 28(8):1769-1782.
11. Geng Y, *et al.* (2013) A spatio-temporal understanding of growth regulation during the salt stress response in Arabidopsis. *The Plant Cell* 25(6):2132-2154.
12. Takahashi N, Goto N, Okada K, & Takahashi H (2002) Hydrotropism in abscisic acid, wavy, and gravitropic mutants of Arabidopsis thaliana. *Planta* 216(2):203-211.
13. Antoni R, *et al.* (2013) PYRABACTIN RESISTANCE1-LIKE8 plays an important role for the regulation of abscisic acid signaling in root. *Plant Physiology* 161(2):931-941.
14. Barberon M, *et al.* (2016) Adaptation of Root Function by Nutrient-Induced Plasticity of Endodermal Differentiation. *Cell* 164(3):447-459.

15. Ondzighi-Assoume CA, Chakraborty S, & Harris JM (2016) Environmental Nitrate Stimulates Abscisic Acid Accumulation in Arabidopsis Root Tips by Releasing It from Inactive Stores. *The Plant Cell* 28(3):729-745.
16. Irigoyen ML, *et al.* (2014) Targeted degradation of abscisic acid receptors is mediated by the ubiquitin ligase substrate adaptor DDA1 in Arabidopsis. *The Plant Cell* 26(2):712-728.
17. Bueso E, *et al.* (2014) The single-subunit RING-type E3 ubiquitin ligase RSL1 targets PYL4 and PYR1 ABA receptors in plasma membrane to modulate abscisic acid signaling. *The Plant Journal* 80(6):1057-1071.
18. Swarup R, *et al.* (2005) Root gravitropism requires lateral root cap and epidermal cells for transport and response to a mobile auxin signal. *Nature Cell Biology* 7(11):1057-1065.
19. Zhang H, *et al.* (2010) ABA promotes quiescence of the quiescent centre and suppresses stem cell differentiation in the Arabidopsis primary root meristem. *The Plant Journal* 64(5):764-774.
20. Belda-Palazon B, *et al.* (2016) FYVE1/FREE1 Interacts with the PYL4 ABA Receptor and Mediates its Delivery to the Vacuolar Degradation Pathway. *The Plant Cell* 28 (9):2178-2196.
21. Yu F, *et al.* (2016) ESCRT-I Component VPS23A Affects ABA Signaling by Recognizing ABA Receptors for Endosomal Degradation. *Molecular Plant* 9(12):1570-1582.
22. Santiago J, *et al.* (2009) Modulation of drought resistance by the abscisic acid receptor PYL5 through inhibition of clade A PP2Cs. *The Plant Journal* 60(4):575-588.
23. Szostkiewicz I, *et al.* (2010) Closely related receptor complexes differ in their ABA selectivity and sensitivity. *The Plant Journal* 61(1):25-35.
24. Okamoto M, *et al.* (2013) Activation of dimeric ABA receptors elicits guard cell closure, ABA-regulated gene expression, and drought tolerance. *Proc Natl Acad Sci USA* 110(29):12132-12137.
25. Cao M, *et al.* (2013) An ABA-mimicking ligand that reduces water loss and promotes drought resistance in plants. *Cell Research* 23(8):1043-1054.
26. Castillo MC, *et al.* (2015) Inactivation of PYR/PYL/RCAR ABA receptors by tyrosine nitration may enable rapid inhibition of ABA signaling by nitric oxide in plants. *Sci.Signal.* 8: ra89.
27. Wu S & Gallagher KL (2014) The movement of the non-cell-autonomous transcription factor, SHORT-ROOT relies on the endomembrane system. *The Plant Journal* 80(3):396-409.
28. Nakajima K, Sena G, Nawy T, & Benfey PN (2001) Intercellular movement of the putative transcription factor SHR in root patterning. *Nature* 413(6853):307-311.
29. Gallagher KL, Paquette AJ, Nakajima K, & Benfey PN (2004) Mechanisms regulating SHORT-ROOT intercellular movement. *Current Biology* 14(20):1847-1851.
30. Palfy M, Remenyi A, & Korcsmaros T (2012) Endosomal crosstalk: meeting points for signaling pathways. *Trends Cell Biology* 22(9):447-456.
31. Christmann A, Hoffmann T, Teplova I, Grill E, & Muller A (2005) Generation of active pools of abscisic acid revealed by in vivo imaging of water-stressed Arabidopsis. *Plant Physiology* 137(1):209-219.
32. Kim TH, *et al.* (2011) Chemical genetics reveals negative regulation of abscisic acid signaling by a plant immune response pathway. *Current Biology* 21(11):990-997.
33. Waadt R, *et al.* (2014) FRET-based reporters for the direct visualization of abscisic acid concentration changes and distribution in Arabidopsis. *eLife* 3:e01739.

34. Jones AM, *et al.* (2014) Abscisic acid dynamics in roots detected with genetically encoded FRET sensors. *eLife* 3:e01741.
35. Zhao Y, *et al.* (2014) The ABA receptor PYL8 promotes lateral root growth by enhancing MYB77-dependent transcription of auxin-responsive genes. *Science signaling* 7(328):ra53.
36. Peirats-Llobet M, *et al.* (2016) A Direct Link between Abscisic Acid Sensing and the Chromatin-Remodeling ATPase BRAHMA via Core ABA Signaling Pathway Components. *Molecular Plant* 9(1):136-147.
37. Moes D, Himmelbach A, Korte A, Haberer G, & Grill E (2008) Nuclear localization of the mutant protein phosphatase *abi1* is required for insensitivity towards ABA responses in Arabidopsis. *The Plant Journal* 54(5):806-819.
38. Lynch, T., Erickson, B. J., and Finkelstein, R. R. (2012). Direct interactions of ABA-insensitive(ABI)-clade protein phosphatase(PP)2Cs with calcium-dependent protein kinases and ABA response element-binding bZIPs may contribute to turning off ABA response. *Plant Mol.Biol.* 80:647-658.

Figure legends.

Fig. 1. ABA treatment specifically increases PYL8 protein levels in seedlings. (A) Effect of CHX, MG132 or ABA treatment on protein levels of HA-tagged receptors. 10-d-old seedlings expressing HA-tagged receptors were either mock- or chemically-treated with 50 μ M CHX, MG132 or ABA for 6 h. Immunoblot analysis using anti-HA was performed to quantify protein levels. * indicates $P < 0.05$ (Student's t test) compared to the corresponding mock-treated sample. (B) Effect of ABA treatment on GFP-PYL2, GFP-PYL4 and GFP-PYL8 protein levels. Seedlings expressing GFP-tagged PYL proteins were either mock- or 50 μ M ABA-treated for 6 h. Immunoblot analysis using anti-GFP was performed to quantify protein levels. (C) ABA treatment leads to selective accumulation of GFP-PYL8 in the nucleus. CLSM analysis of Arabidopsis root differentiation zone in lines expressing GFP-tagged PYL proteins that were either mock- or ABA-treated for 1 h. Scale bars=30 μ m.

Fig. 2. ABA increases PYL8 protein levels in roots through a posttranscriptional mechanism. (A) PYL8-GFP complements the ABA-insensitive *pyl8-1* phenotype. 5-d-old seedlings germinated on MS plates were transferred to new plates lacking or supplemented with 10 μ M ABA and quantification of root growth was performed after 10 d. Data are averages \pm SD from three independent experiments (n=20). * indicates $P < 0.05$ (Student's t test) compared to Col-0 in the same assay conditions. (B) ABA treatment leads to accumulation of PYL8-GFP protein and down-regulation of *PYL8-GFP* mRNA

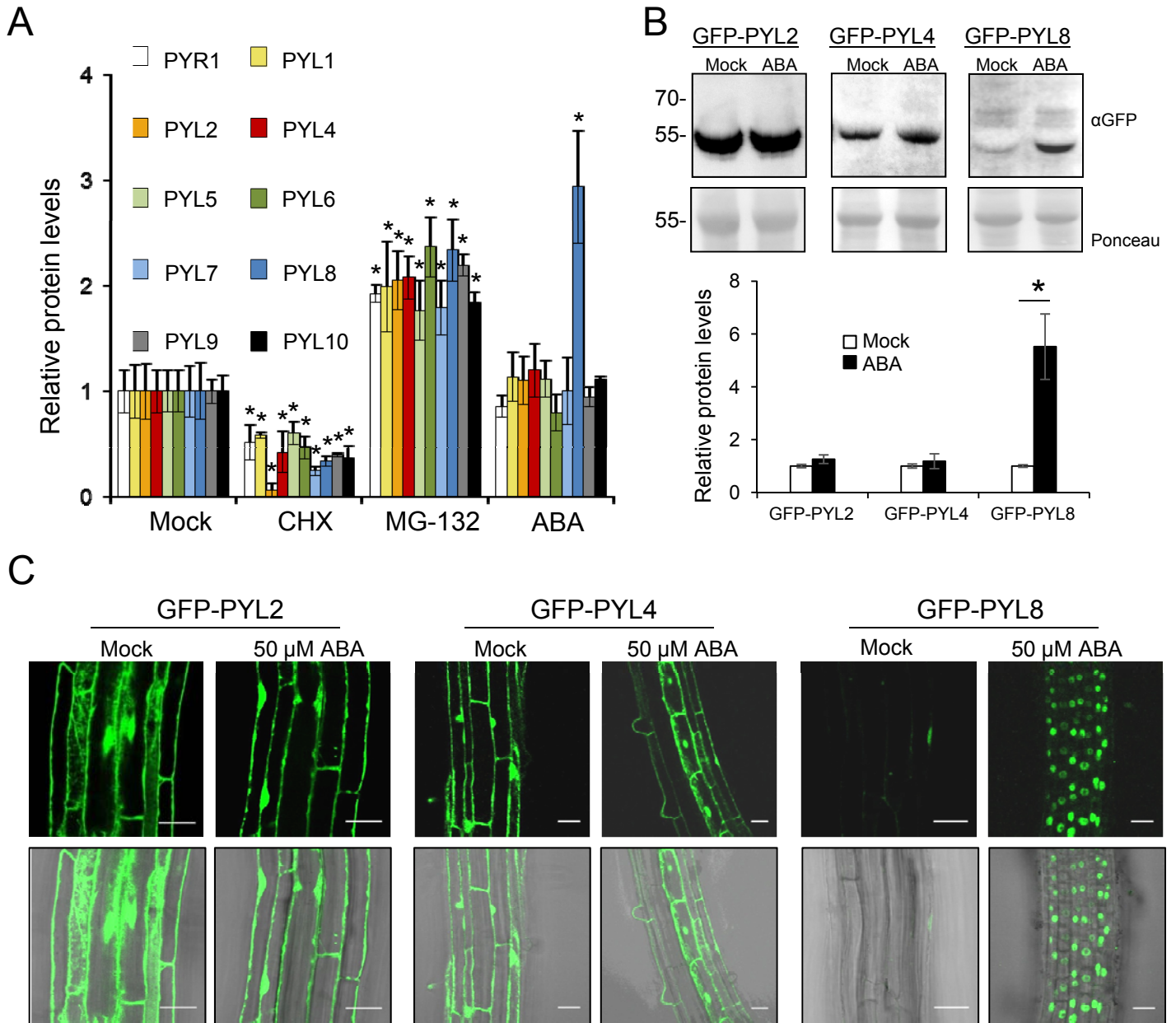
in roots. 10-d-old seedlings expressing PYL8-GFP were either mock- or 50 μ M ABA-treated for 3 h and protein or RNA extracted from root tissue. Immunoblot analysis using anti-GFP was performed to quantify protein levels of PYL8-GFP (asterisk) in roots. A major 30 kDa root protein was used to normalize protein loading. qRT-PCR analyses were performed to quantify mRNA expression of PYL8-GFP. * indicates $P < 0.05$ (Student's t test) compared to mock-treated samples. (C) ABA treatment leads to accumulation of PYL8-GFP in the nucleus. CLSM analysis of Arabidopsis root expressing ProPYL8:PYL8-GFP in the *pyl8-1* background after mock- or ABA-treatment for 6 h. Scale bars=25 μ m. (D) Dose-response analysis of PYL8-GFP accumulation in response to treatment with the indicated ABA concentrations for 6h. Fluorescence was quantified in arbitrary units (a.u.) using images acquired by CLSM. (E) Accumulation of PYL8-GFP after 250 mM sorbitol treatment. Fluorescence was measured after treatment with 125 mM or 250 mM sorbitol (S) or 50 μ M ABA for 3 h. Scale bars=30 μ m. * indicates $P < 0.05$ (Student's t test) compared to mock-treated samples.

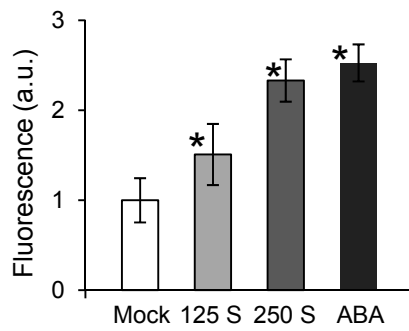
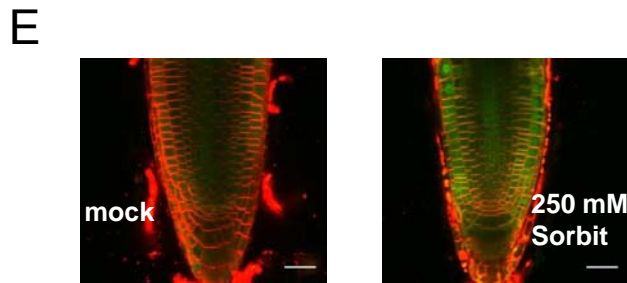
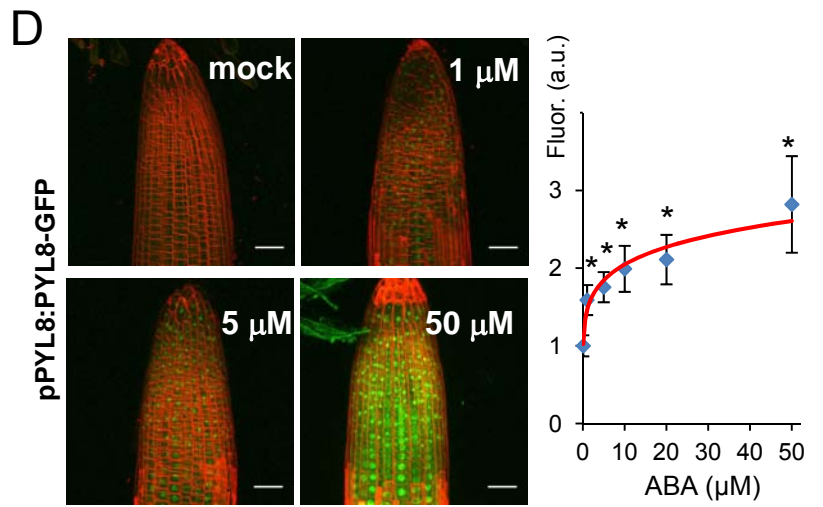
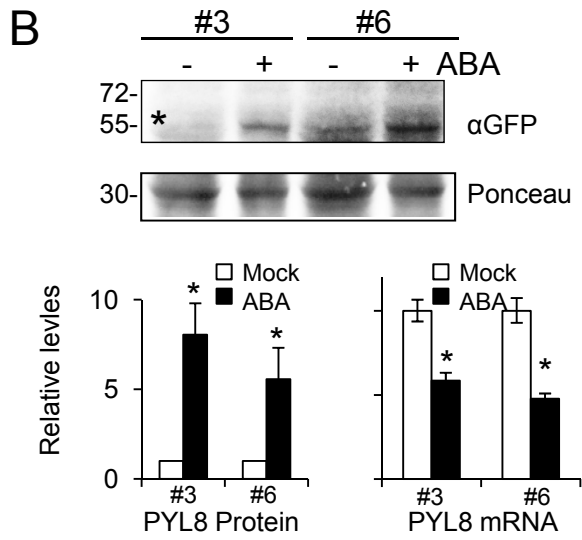
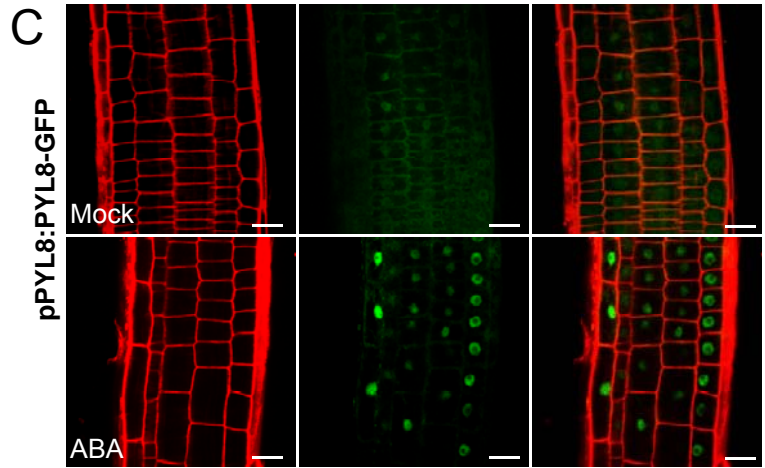
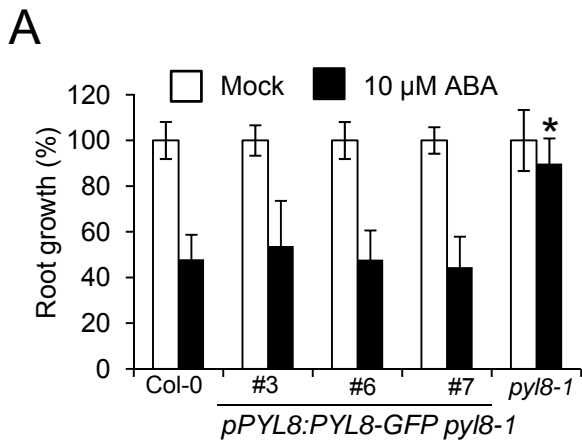
Fig. 3. ABA perception by PYL8 is required to trigger its stabilization via reduced receptor ubiquitination. (A) QB treatment does not lead to accumulation of PYL8-GFP. QB induces ABA signaling in the root as revealed by the pRAB18:GFP reporter. CLSM analysis of Arabidopsis root apex expressing either ProPYL8:PYL8-GFP in the *pyl8-1* background or ProRAB18:GFP in wt after mock-, 20 μ M ABA- or 50 μ M QB-treatment for 1 h. * indicates $P < 0.05$ (Student's t test) compared to mock (DMSO)-treated sample. (B) ABA prevents degradation of PYL8-GFP in roots whereas QB does not. 10-d-old seedlings expressing PYL8-GFP were treated with 50 μ M ABA for 6 h to induce accumulation of PYL8. After washing out ABA, a CHX treatment in the absence or presence of 50 μ M ABA or QB was performed for 60 or 120 min. Protein extracts of roots were analyzed using an anti-GFP antibody (α -GFP). The histogram shows the quantification of the PYL8-GFP protein during the CHX treatment. * indicates $P < 0.05$ (Student's t test) when CHX+ABA treatment was compared to CHX or CHX+QB treatments, respectively. (C) ABA treatment increases total HA-PYL8 protein levels in root but reduces polyubiquitinated PYL8 forms. Protein extracts were prepared from mock or ABA-treated root

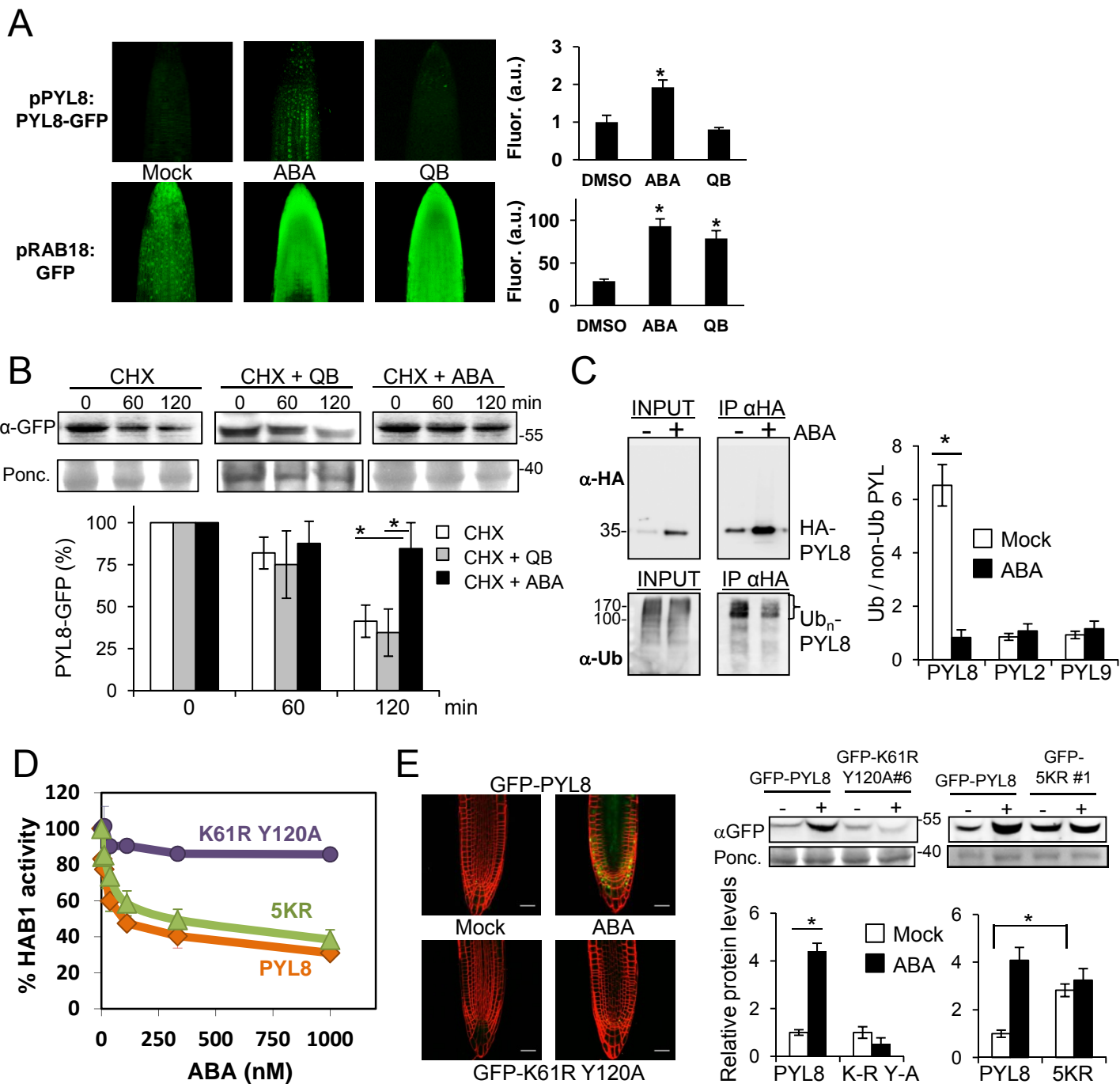
samples and submitted to immunoprecipitation using anti-HA antibodies. Immunoprecipitated PYL8 (IP α HA) was analyzed by immunoblotting using anti-HA and anti-Ub (P4D1) antibodies. The ratio of polyubiquitinated to non-Ub PYL8, PYL2 and PYL9 protein was quantified in mock- and ABA-treated samples. * indicates $P < 0.05$ (Student's t test) compared to ABA-treated sample. (D) The PYL8^{K61R Y120A} mutant is unable to inhibit PP2C HAB1, whereas activity of PYL8^{5KR} is similar to PYL8 wt. Phosphatase activity of HAB1 was measured in the presence of PYL8 wt, PYL8^{K61R Y120A} or PYL8^{5KR} mutants and different ABA concentrations. (E) CLSM of Arabidopsis root apex (left panels) and immunoblot analysis of root protein extracts reveal that the PYL8^{K61R Y120A} mutant is not stabilized by ABA. Transgenic seedlings expressing GFP-PYL8, GFP-PYL8^{K61R Y120A} or GFP-PYL8^{5KR} were either mock- or 50 μ M ABA-treated for 3 h, root protein extracts were prepared and immunoblot analysis was performed using anti-GFP to quantify protein levels (right panels). * indicates $P < 0.05$ (Student's t test) when the indicated samples were compared.

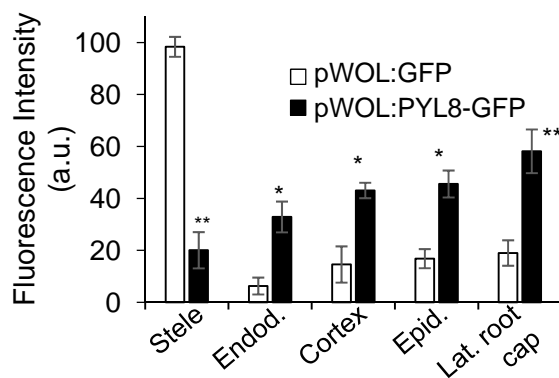
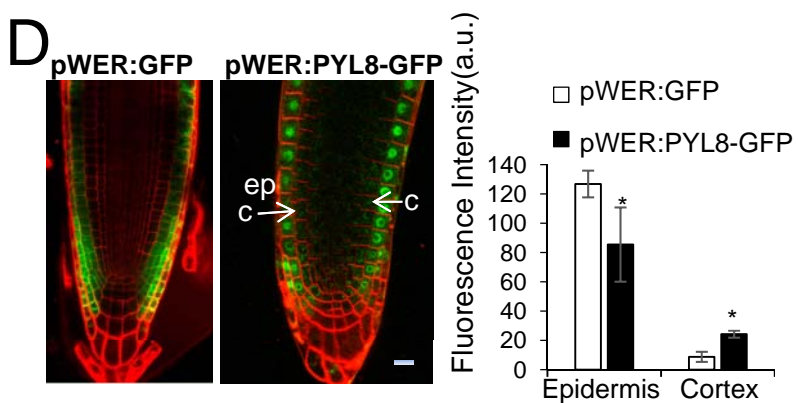
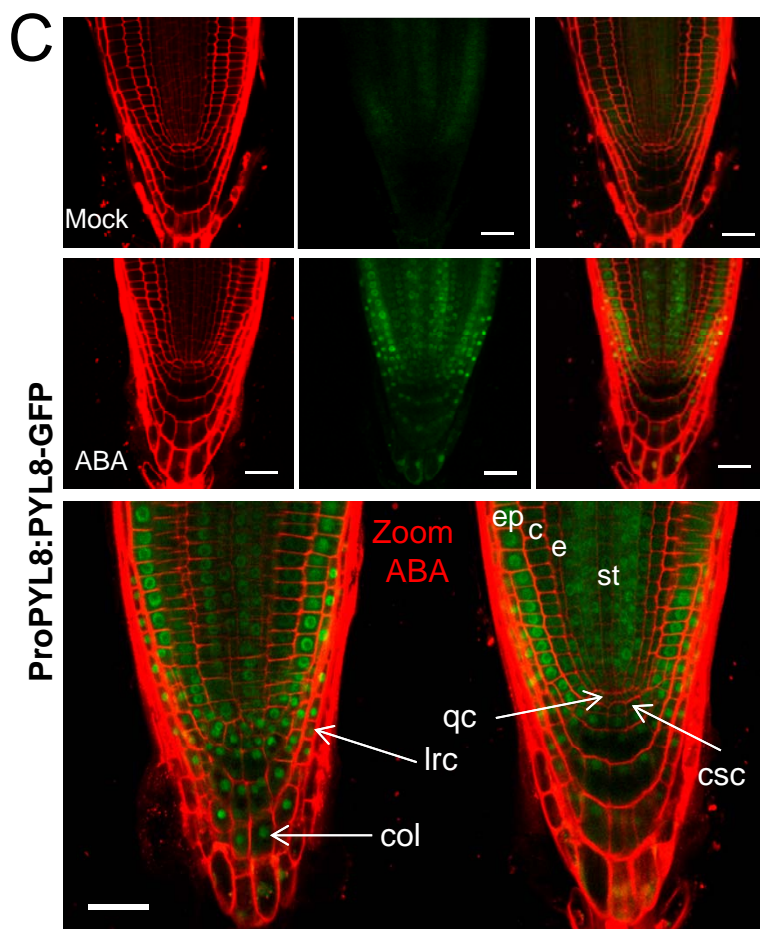
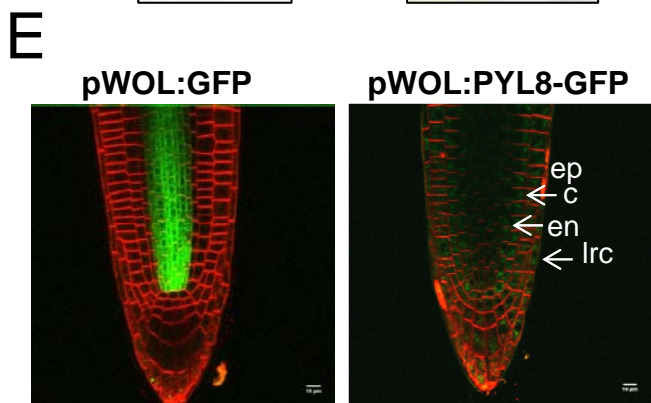
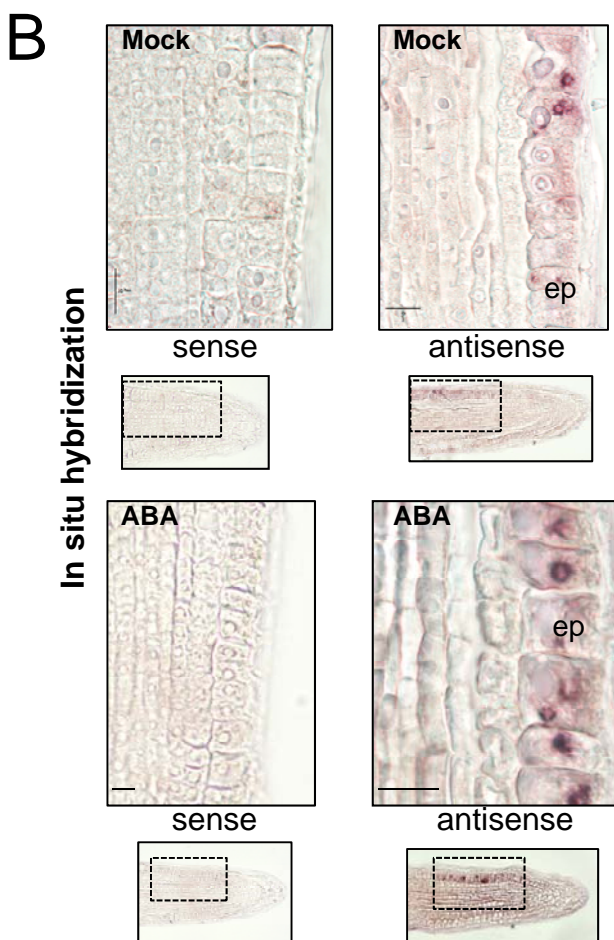
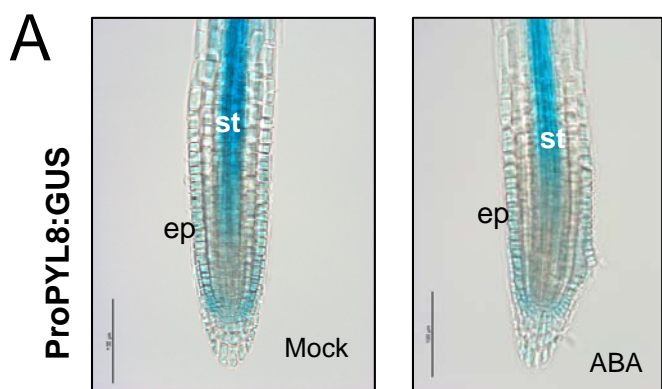
Fig. 4. Expression of PYL8 transcript and protein in roots. (A) GUS expression driven by the ProPYL8:GUS gene in the root apex. GUS staining after mock- or 50 μ M ABA treatment. Scale bars=100 μ m (B) Localization of *PYL8* mRNA in the root apex. *In situ* hybridization was performed on longitudinal sections of the root apex of mock- or 50 μ M ABA-treated seedlings using *PYL8* antisense or sense probes. The *PYL8* transcript was visualized using anti digoxigenin-AP antibody and NBT/BCIP staining. Scale bars=10 μ m. (C) CSLM visualization of PYL8-GFP driven by the PYL8 promoter after mock- or ABA-treatment. Localization of PYL8-GFP after ABA treatment was detected in the root apical meristem, columella and lateral root cap. Scale bars=25 μ m. Abbreviations: ep, epidermis; c, cortex; e, endodermis; st, stele; qc, quiescent center; lrc, lateral root cap; col, columella; csc, columella stem cells. (D-E) CSLM visualization of GFP or PYL8-GFP proteins expressed under the control of the *pWER* and *pWOL* promoters in *pyl8-2* background. In order to stabilize PYL8, seedlings were treated with 50 μ M MG132 and ABA for 6 h. Scale bars=10 μ m. Histograms indicate tissue-scale measurements of CLSM images using CellSeT software. * indicates $P < 0.05$ and ** $P < 0.01$ (Student's t test) compared to GFP control.

Fig. 5. Proposed model for ABA-dependent stabilization and movement of the non-cell-autonomous ABA receptor PYL8. (A) PYL8 translocation from epidermis (blue arrows) and stele (red arrows) to adjacent tissues. Translocation could be promoted by increased ABA levels or follow a default mechanism that is reinforced by ABA-induced accumulation of PYL8. The intercellular movement of PYL8 is accompanied by intracellular trafficking and increased nuclear accumulation in response to ABA. (B) ABA reduces polyubiquitination of PYL8 through an unknown mechanism, which stabilizes and increases PYL8 protein levels. ABA also enhances PYL8 localization in the nucleus (n), which prevents vacuolar degradation and might represent an additional mechanism to increase PYL8 levels.












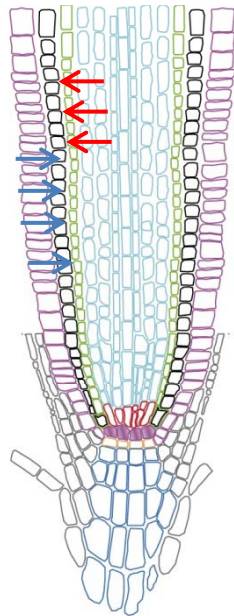




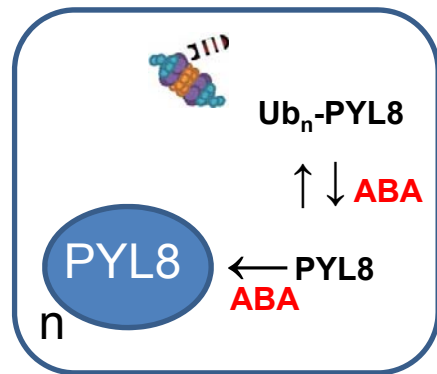


A

-  LRC
-  Columella
-  Epidermis
-  Cortex
-  Endodermis
-  Stele
-  Vascular initials
-  Quiescent center
-  Columella stem cells



B



Supplementary Information for

PYL8 mediates ABA perception in the root through non-cell-autonomous and ligand stabilization based mechanisms

Borja Belda-Palazon¹, Mary-Paz Gonzalez-Garcia², Jorge Lozano-Juste¹, Alberto Coego¹, Regina Antoni¹, Jose Julian¹, Marta Peirats-Llobet¹, Lesia Rodriguez¹, Ana Berbel¹, Daniela Dietrich³, Maria A. Fernandez¹, Francisco Madueño¹, Malcolm J. Bennett³, and Pedro L. Rodriguez*¹

Corresponding author: Pedro L. Rodriguez*¹

Email: prodriguez@ibmcp.upv.es

This PDF file includes:

SI Materials and methods
Figs. S1 to S6
Table S1
Captions for movies S1 to S2
SI references

Other supplementary materials for this manuscript include the following:

Movies S1 to S2

SI Materials and methods

Plant material and growth conditions. *Arabidopsis thaliana* plants were routinely grown under greenhouse conditions (40-50% relative humidity) in pots containing a 1:3 vermiculite-soil mixture. For plants grown under growth chamber conditions, seeds were surface sterilized by treatment with 70% ethanol for 20 min, followed by commercial bleach (2.5 % sodium hypochlorite) containing 0.05 % Triton X-100 for 10 min, and finally, four washes with sterile distilled water. Stratification of the seeds was conducted in the dark at 4°C for 3 days. Seeds were sowed on Murashige-Skoog (MS) plates composed of MS basal salts, 0.1% 2-[N-morpholino]ethanesulfonic acid, 1% sucrose and 1% agar. The pH was adjusted to 5.7 with KOH before autoclaving. Plates were sealed and incubated in a controlled environment growth chamber at 22°C under a 16 h light, 8 h dark photoperiod at 80-100 $\mu\text{E m}^{-2} \text{sec}^{-1}$.

Generation of HA-tagged and GFP-tagged receptor lines and ProPYL8:PYL8-GFP *pyl8-1* lines. HA-tagged PYR1/PYL4/PYL5/PYL8 transgenic lines have been described previously (1, 2, 3). HA-tagged PYL1/PYL2/PYL6/PYL7/PYL9/PYL10/PYL8^{5KR} constructs were done in pAlligator2 and transgenic lines were generated as described (3). GFP-PYL4 transgenic line has been described previously (4). GFP-PYL2, GFP-PYL8 and GFP-PYL8^{K61R Y120A} and GFP-PYL8^{5KR} constructs were done in the pMDC43 vector and transgenic lines were generated as described (4). The PYL8^{K61R, Y120A} mutant was generated using overlap extension by PCR and SLIM-PCR procedures (see below for details) and primers described in Table S1. The PYL8^{5KR} mutant was obtained as a synthetic DNA fragment (see below for details). To express PYL8 under control of its native promoter, a 2.9 kb fragment comprising 2 kb PYL8 promoter and the PYL8 genomic sequence lacking the stop codon was amplified by PCR using primers FproPYL8 and RnostopPYL8 (Table S1). It was cloned into pCR8/GW/TOPO and recombined by Gateway LR reaction into pMDC107 destination vector. The pMDC107-based construct carrying the ProPYL8:PYL8-GFP gene was transferred to *Agrobacterium tumefaciens* pGV2260 by electroporation and used to transform *pyl8-1* plants (phosphinothricin resistant) by the floral dipping method. Seeds of transformed plants were harvested and plated on hygromycin (20 $\mu\text{g/ml}$) selection medium to identify T1

transgenic plants and T3 progenies homozygous for the selection marker were used for further studies.

Expression of PYL8-GFP in root driven by tissue-specific promoters. The PYL8-GFP coding sequence was amplified by PCR from the pMDC83_PYL8-GFP template using the primers FwPstIPYL8 and RvBamHIGFP. Next, it was cloned into pCR8/GW/TOPO, verified by sequencing and recombined by Gateway LR reaction into pWOL_GW destination vector, which drives expression of PYL8-GFP in root vascular cylinder and pericycle (5). Additionally, PYL8-GFP was excised using a *PstI-BamHI* double digestion and cloned into pG0229-T WER, which drives expression in epidermis and lateral root cap (6). The resulting constructs pWOL:PYL8-GFP and pG0229-T WER:PYL8-GFP were transferred to *Agrobacterium tumefaciens* pGV2260 by electroporation and used to transform Col-0 and *pyl8-2* (kanamycin resistant) plants by the floral dipping method. Seeds of transformed plants were harvested and plated on phosphinothricin (20 μ M) selection medium to identify T1 transgenic plants and T3 progenies homozygous for the selection marker were used for further studies.

Generation of PYL8 mutations. The K61R mutation was introduced into PYL8 coding sequence by overlap-extension PCR using the primers FK61R and RK61R, cloning into pCR8/GW/TOPO and verification by sequencing. Next, the PYL8^{K61R} coding sequence was excised using an *NcoI-EcoRI* double digestion and cloned into pETM11 to obtain recombinant protein. SLIM-PCR (7) was used to generate the Y120A mutation into the pETM11-PYL8^{K61R} template using the following primers: PYL8Y120A-F3, PYL8Y120A-FT3, PYL8Y120A-R3 and PYL8Y120A-RT3 (Table S1). Next, the PYL8^{K61R Y120A} coding sequence was cloned into pCR8/GW/TOPO, verified by sequencing and subsequently recombined using LR Gateway into pMDC43 vector. The quintuple Lys-Arg PYL8 mutant (Lys24Arg, Lys38Arg, Lys59Arg, Lys70Arg and Lys84Arg) was obtained as a synthetic DNA fragment (Invitrogen), which was amplified using Fpyl8-1*NcoI* and RvStop PYL8 primers and cloned into pCR8/GW/TOPO, verified by sequencing and subsequently recombined into pMDC43 and pAlligator2. PYL8^{5KR} coding sequence was excised using an *NcoI-EcoRI* double digestion from pCR8/GW/TOPO and cloned into pETM11 to obtain recombinant protein.

In vivo protein analysis and degradation assay. Surface sterilized seeds of transgenic lines overexpressing HA-tagged or GFP-tagged PYR/PYL receptors were sown in MS plates and grown for 4 days. Seedlings were transferred to liquid culture and grown for 10 days in 2 mL of liquid MS medium. Then, they were either mock-treated or incubated with 50 μ M MG132, 50 μ M ABA or 50 μ M MG132+50 μ M ABA for 6h. Plant material was collected and frozen in liquid nitrogen at the indicated times. When indicated roots were sectioned and used to prepare protein extracts. Plant material (0.1 g) was extracted in 2 volumes of 50 mM Tris-HCl, pH 8.0, 150 mM NaCl, 1% Triton X-100, 3 mM DTT and 1x Complete Protease Inhibitor Cocktail (Roche). After protein quantification of each plant extract, 10 μ g of total protein was loaded on a 10% SDS-PAGE gel. Proteins were transferred onto Immobilon-P membranes (Millipore) and probed with anti-HA horseradish peroxidase (HRP) antibody (Roche; 1:1000 dilution) or an anti-GFP monoclonal antibody (clone JL-8; Clontech; 1:10000 dilution) as primary antibody and ECL anti-mouse peroxidase (GE Healthcare; 1:5000 dilution) as secondary antibody. Detection was performed using the ECL select Western blotting detection kit (GE Healthcare). Image capture was done using a cooled CCD camera system and the image analyzer LAS3000 and quantification of the protein signal was done using Image Guache V4.0 software. The signal intensities of the digitalized images were quantified using Image-Gauge version 4.0 using Rubisco to normalize protein loading.

The effect of ABA treatment on PYL8-GFP protein levels was analyzed in root tissue of the ProPYL8:PYL8-GFP pyl8-1 transgenic line. Two-week-old plants grown in liquid culture were 50 μ M ABA-treated for 6 h and root tissue was collected and frozen in liquid nitrogen. For the analysis of PYL8-GFP stability, after ABA treatment for 6 h, plants were washed out and then submitted to a 100 μ M CHX chase for 60 or 120 min in the absence or presence of 50 μ M ABA or QB. Root tissue was collected and frozen in liquid nitrogen. Protein extraction was performed as described above and 150 μ g of total protein were analyzed by using the anti-GFP (JL8 clone, Clontech) antibody. The band intensities were quantified as described above. Immunoprecipitation of HA-PYL8 was conducted in protein extracts (2.5 mg total protein) obtained from sectioned roots that were either mock or ABA treated. Protein extracts were incubated with 50 μ L of anti-HA antibody coupled to paramagnetic beads (Miltenyi Biotec) at 4°C for 3 h. The

immunoprecipitated proteins were eluted following the manufacturer's instructions and analyzed using anti-HA-HRP antibody or anti-Ub antibody (P4D1; Santa Cruz Biotechnology; 1:1000 dilution) as primary antibody and ECL anti-mouse peroxidase as secondary antibody.

Root growth assay. Seedlings were grown on vertically oriented Murashige and Skoog plates for 4-5 days. Afterwards, 20 plants were transferred to new plates that lacked or were supplemented 10 μ M ABA. The plates were scanned on a flatbed scanner after 10 days to produce image files suitable for quantitative analysis of root growth using the NIH Image software ImageJ version 1.37. When indicated the total number of lateral roots was also scored in plants grown in medium lacking or supplemented with 10 μ M ABA.

RT-qPCR. RNA was extracted from seedlings that were either mock- or 50 μ M ABA treated using NucleoSpin® RNA Plant kit from Machery-Nagel, following the manufacturer's instructions. cDNA was synthesized from 2 μ g of total purified RNA using 30 U of RevertAid Reverse Transcriptase (Thermo Scientific). RT-qPCR was performed using PyroTaq EvaGreen qPCR Master Mix 5X from CultiGen, which includes EvaGreen® Dye and carboxy-X-rhodamine (ROX) as a passive reference dye. The reaction was performed in a final volume of 10 μ L using 0.4 μ L of cDNA. The primer pairs used for this analysis are listed in Table 1. qPCR was performed in the 7500 Fast Real-Time PCR System from Applied Biosystems.

PP2C inhibition assays. Phosphatase activity was measured using pNPP as a substrate (15 mM), 1 μ M of the PP2C Δ NHAB1 and 2 μ M of the indicated receptors. Dephosphorylation of pNPP was monitored with a ViktorX5 reader at 405 nm (8). Concentrations of 0, 4, 11, 33, 111, 333 and 1000 nM ABA were used for dose-response assays. Values are expressed as percentage of activity with respect to those in the absence of ligand.

GUS staining. The b-glucuronidase histochemical assay was performed basically as described (9). Whole seedlings were submerged in GUS-staining solution: 5-bromo-4-chloro-3-indolylglucuronide (X-Gluc), K⁺ ferricyanide/ ferrocyanide. After GUS staining, roots were clarified in acidified methanol solution, followed by neutralization

and incubation in ethanol. Root GUS staining was also visualized using modified PS-PI staining and CLSM as described previously (9).

RNA in situ hybridization. RNA in situ hybridization with digoxigenin-labelled probes was performed basically as described previously (10). For *in situ* experiments 2 days old WT (Col-0) seedlings were either mock or 50 μ M ABA treated for 6 hours and fixed for 15 minutes under vacuum at room temperature in FAE solution (ethanol:acetic acid:formaldehyde:water, 50:5:3.5:41.5, v/v/v/v). The FAE solution was refreshed and the samples were incubated for additional 16 hours at 4°C. Afterwards, the seedlings were dehydrated, paraffin-embedded and sectioned to 7 μ m. After dewaxing in histoclear and rehydration, sections were treated for 20 minutes in 0.2 M HCl, neutralized for 10 minutes in 2' SSC and incubated for 30 minutes with 1 mg/ml Proteinase K at 37°C. Proteinase action was blocked with 5 minutes incubation in 2 mg/ml Gly and 10 minutes postfixation in 4% formaldehyde. Tissue sections were washed in PBS, dehydrated through an ethanol series and dried under vacuum before applying the hybridization solution (100 mg/ml tRNA; 6' SSC; 3% SDS; 50% formamide, containing approx. 100 ng/ml of antisense DIG-labeled RNA probe). Sections were hybridized overnight at 52°C, washed twice for 90 minutes in 2' SSC; 50% formamide at 53°C and the DIG-antibody incubation and color detection with NBT-BCIP as substrates was performed according to the manufacturer instructions (Boehringer).

The PYL8 RNA antisense and sense probes were generated using as template the 253-bp fragment of the PYL8 coding sequence comprising nucleotides 507-760, which was amplified by PCR and cloned in both orientations into the EcoRI site of pBluescript[®] SK (+/-)vector. Antisense and sense RNA probes were obtained by *in vitro* transcription using the T7 RNA polymerase and labeling with digoxigenin-UTP (Roche).

CLSM. Confocal imaging was performed using a Zeiss LSM 780 AxioObserver.Z1 laser scanning microscope with C-Apochromat 40x/1.20 W corrective water immersion objective. The following dyes or fluorophores were used: Propidium iodide (Sigma-Aldrich), at a final concentration of 10 μ g/mL (561 nm/600-660 nm); FM4-64 (SynaptoRed[™], Biotium), at a final concentration of 10 μ M (561 nm/620-700 nm); GFP (488 nm/500-530 nm). Pinholes were adjusted to 1 Air Unit for each wavelength. For the

GFP quantitative z-scan analysis of the roots the power of the 488 nm laser was set at 3.0% transmission to gain master of 830. If not specified, sections of 55 μm were analyzed compiling 23 slices with an interval of 2.50 μm . Post-acquisition image processing was performed using ZEN (ZEISS Efficient Navigation) Lite 2012 imaging software and ImageJ (<http://rsb.info.gov/ij/>).

Measurements and statistical analysis. Primary root length was measured with the ImageJ software. Tissue-scale measurements of CLSM images were performed using CellSeT software (11) available from <https://www.cpiib.ac.uk/tools-resources/software/cellset/>. Significant differences were calculated using Student's T-test for single comparisons and Tukey HSD test for multiple comparisons (* $p < 0.05$; ** $p < 0.01$). Values are averages obtained from three independent experiments \pm SD.

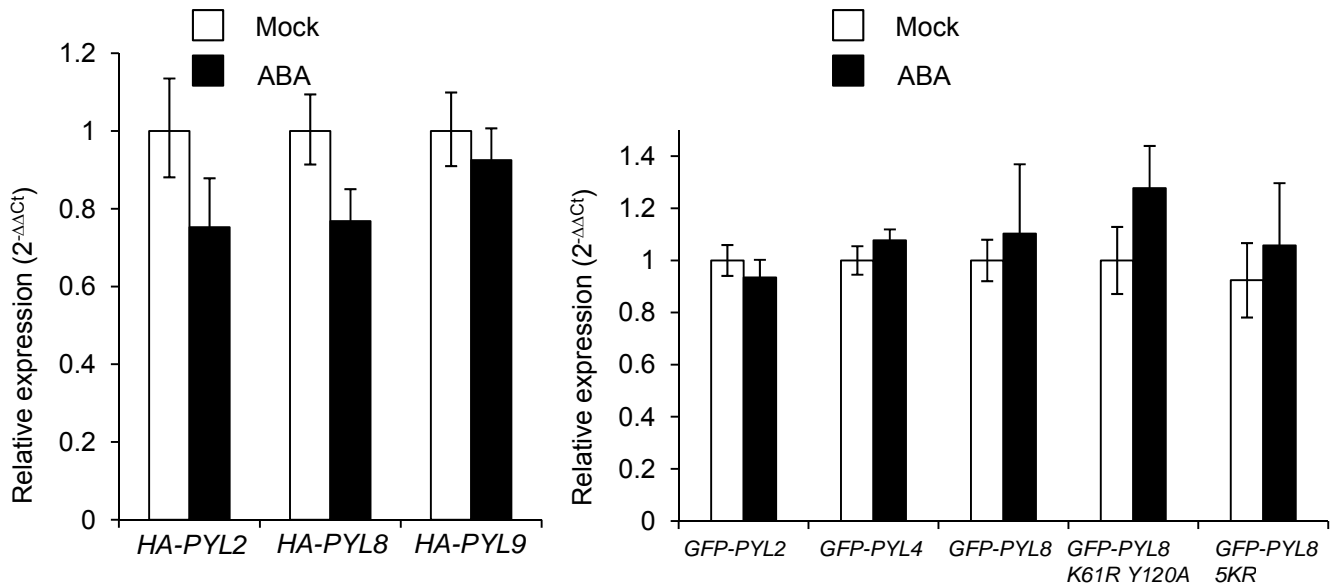


Fig. S1. Expression of 35S:HA-PYL and 35S:GFP-PYL transcripts is not significantly affected by ABA treatment. Data are averages \pm SD from three independent experiments. RNA was extracted from seedlings that were either mock- or 50 μ M ABA treated. RT-qPCR analyses from the indicated transcripts were performed using *actin-8* to normalize data.

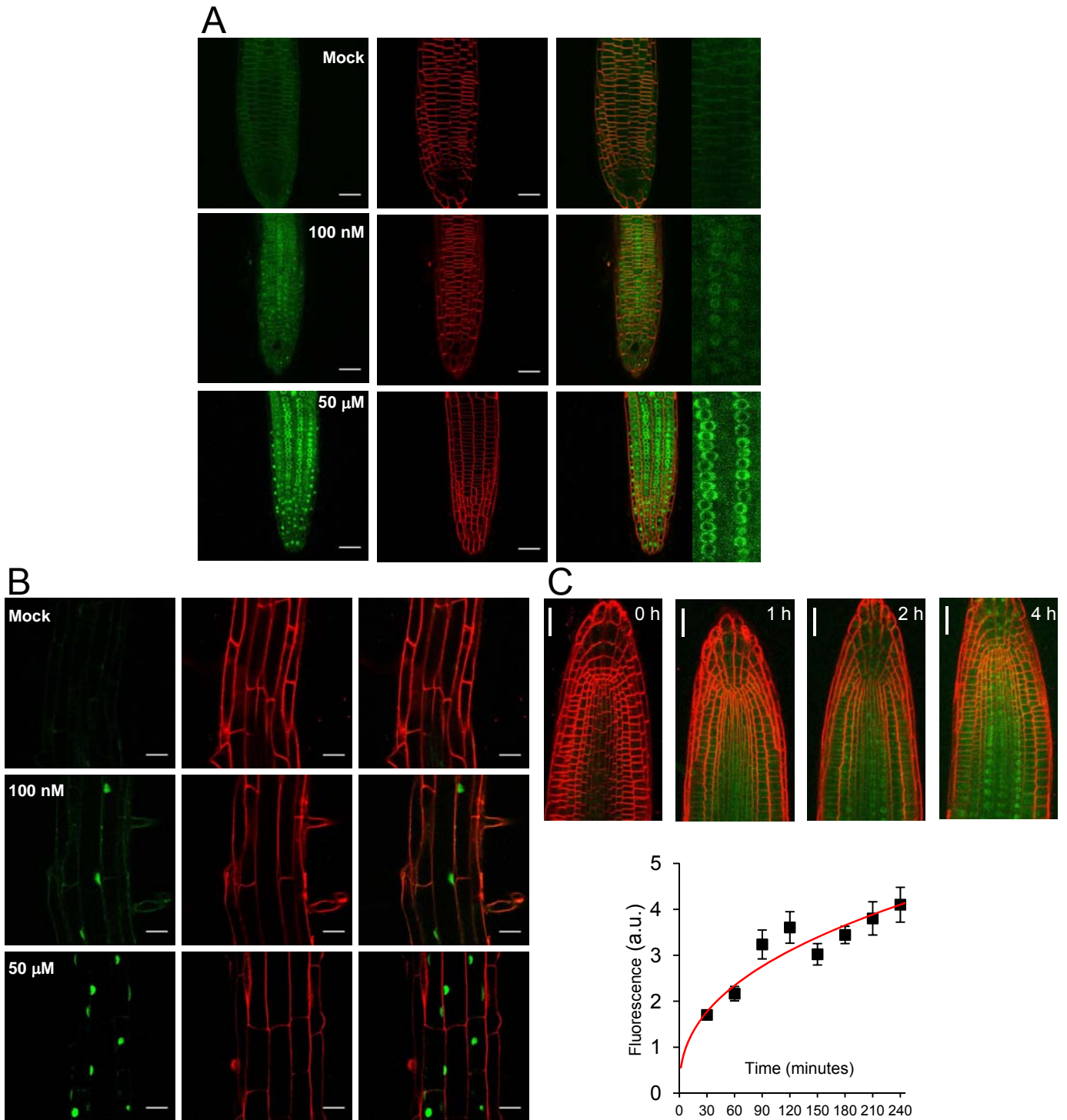


Fig. S2. Dose-response and kinetic analysis of PYL8-GFP accumulation in response to ABA. (A) Perception of nM ABA concentration by PYL8-GFP in the epidermis of the root apex. Scale bars=30 μm . Close-up view highlighting the enhanced nuclear accumulation of PYL8 at higher ABA concentration (right panels). (B) Perception of nM ABA concentration by PYL8-GFP in mature root. After 50 μM ABA-treatment for 6h, most of PYL8 is localized in nucleus whereas at 100 nM ABA cytosolic localization is also apparent. (C) Kinetic analysis of PYL8 accumulation in the root apex in response to 10 μM ABA.

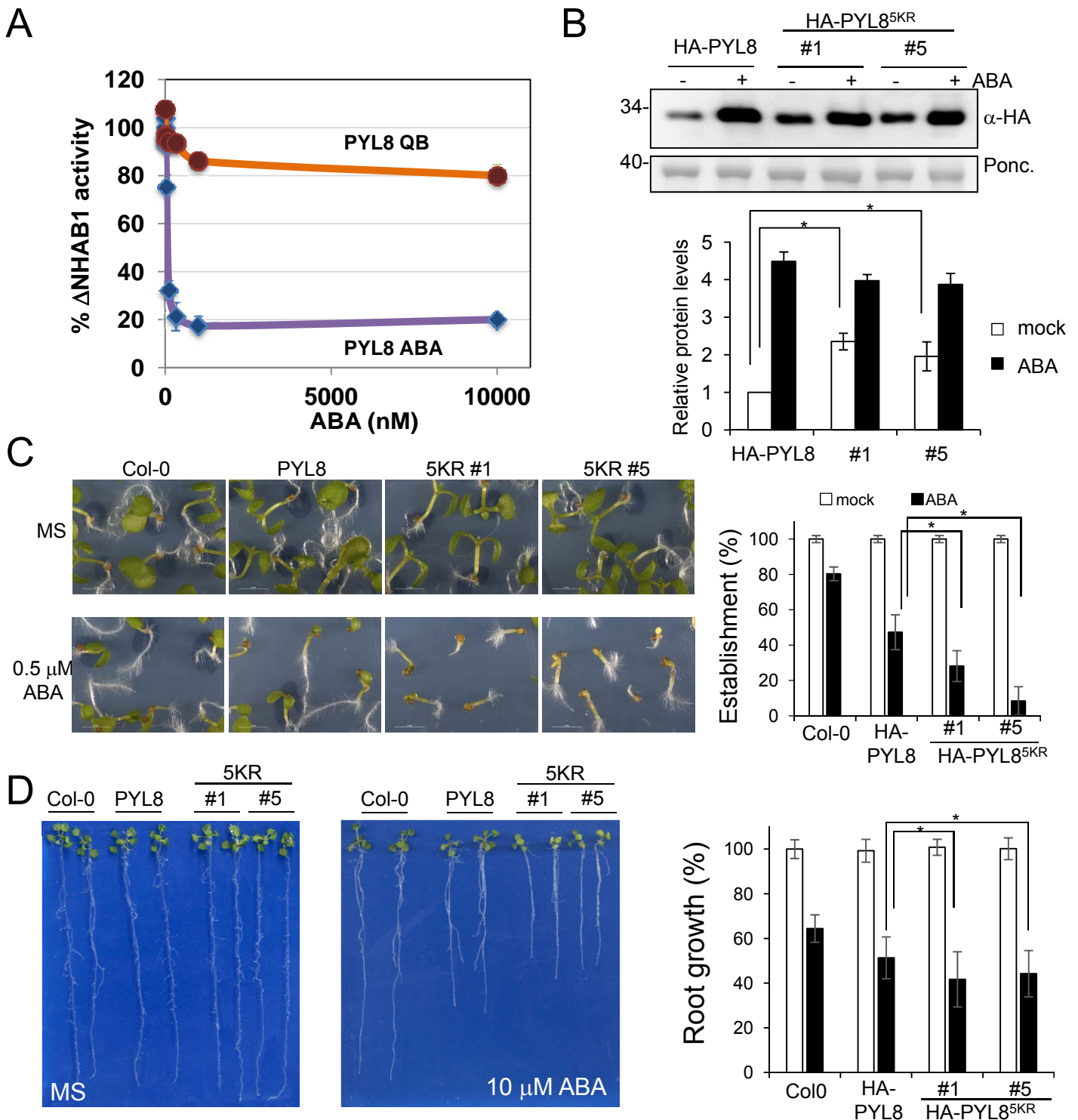


Fig S3. The $PYL8^{5KR}$ mutant shows enhanced stabilization compared to wild-type $PYL8$ at endogenous ABA levels. (A) QB does not significantly inhibit $PYL8$. Phosphatase activity of $\Delta NHAB1$ (lacking amino acids 1-178) was measured in the presence of $PYL8$ and different concentrations of QB or ABA. (B) Immunoblot analysis reveals higher $PYL8^{5KR}$ levels compared to wild-type $PYL8$ at endogenous ABA concentration. Protein extracts were prepared from mock- or ABA-treated samples obtained from Arabidopsis transgenic plants that express HA-tagged $PYL8$ or $PYL8^{5KR}$. Transgenic seedlings expressing HA- $PYL8$ or HA- $PYL8^{5KR}$ were either mock- or 50 μM ABA-treated for 3 h, root protein extracts were prepared and immunoblot analysis was performed using anti-HA to quantify protein levels (histograms). * indicates $P < 0.05$ (Student's t test) compared to mock-treated sample. (C-D) Enhanced sensitivity to ABA-mediated inhibition of seedling establishment or root growth of Arabidopsis transgenic plants that express $PYL8^{5KR}$ compared to wild-type $PYL8$.

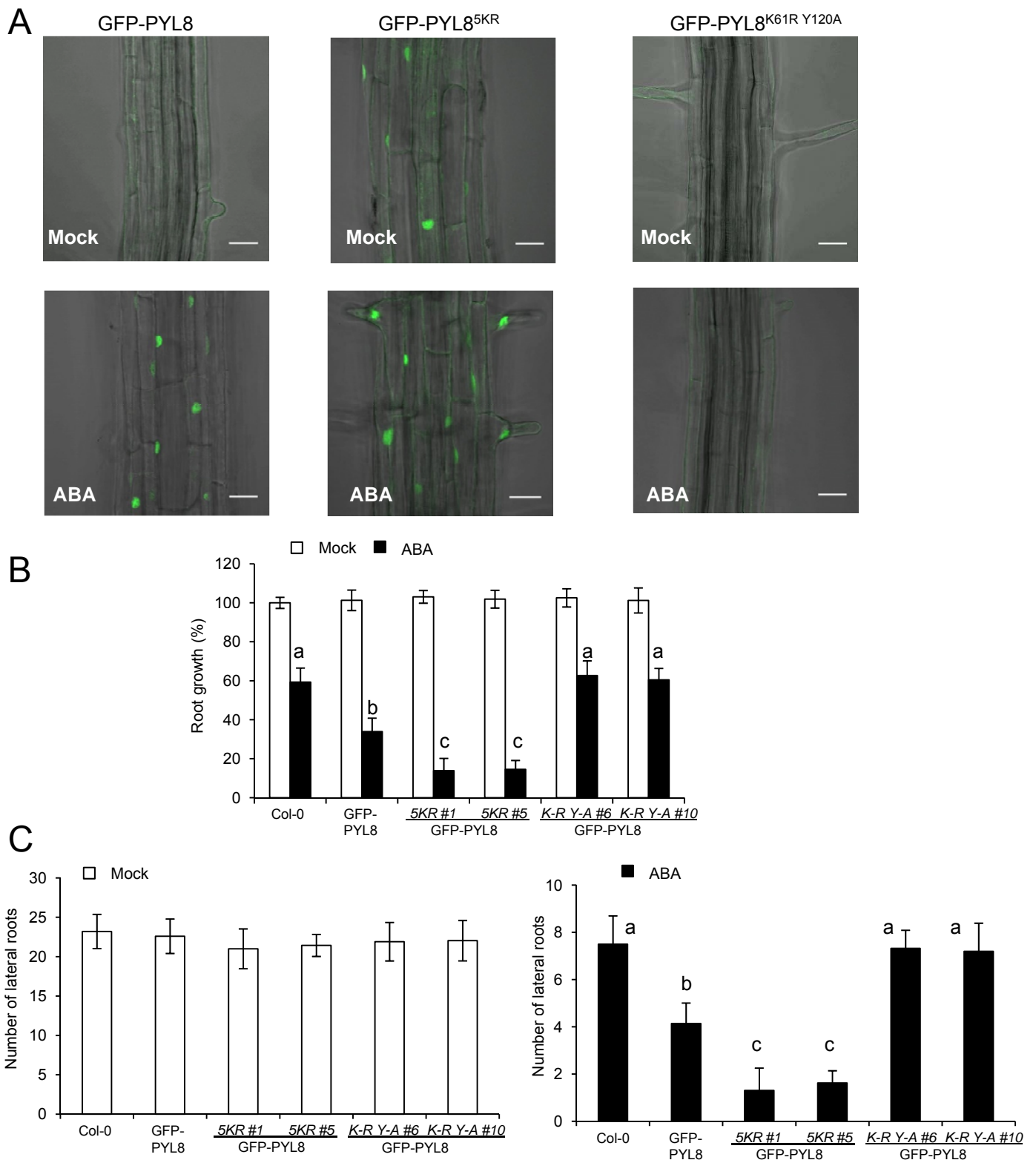


Fig. S4. Nuclear accumulation of PYL8 induced by ABA is required for ABA response. (A) CLSM analysis of Arabidopsis root differentiation zone in lines expressing GFP-PYL8, GFP-PYL8^{5KR} and GFP-PYL8^{K61R Y120A} proteins that were either mock- or 50 μ M ABA-treated for 1 h. Scale bars=30 μ m. Bright field and fluorescent signals are overlapped. (B) ABA-mediated inhibition of root growth in the indicated backgrounds. 5-d-old seedlings germinated on MS plates were transferred to new plates lacking or supplemented with 10 μ M ABA and quantification of root growth was performed after 10 d. Data are averages \pm SD from three independent experiments (n=20). (C) ABA-mediated repression of lateral root formation in the indicated backgrounds. The number of lateral roots was quantified in seedlings from the experiment described above. The different letters denote significant differences among the different genetic backgrounds (Tukey HSD test).

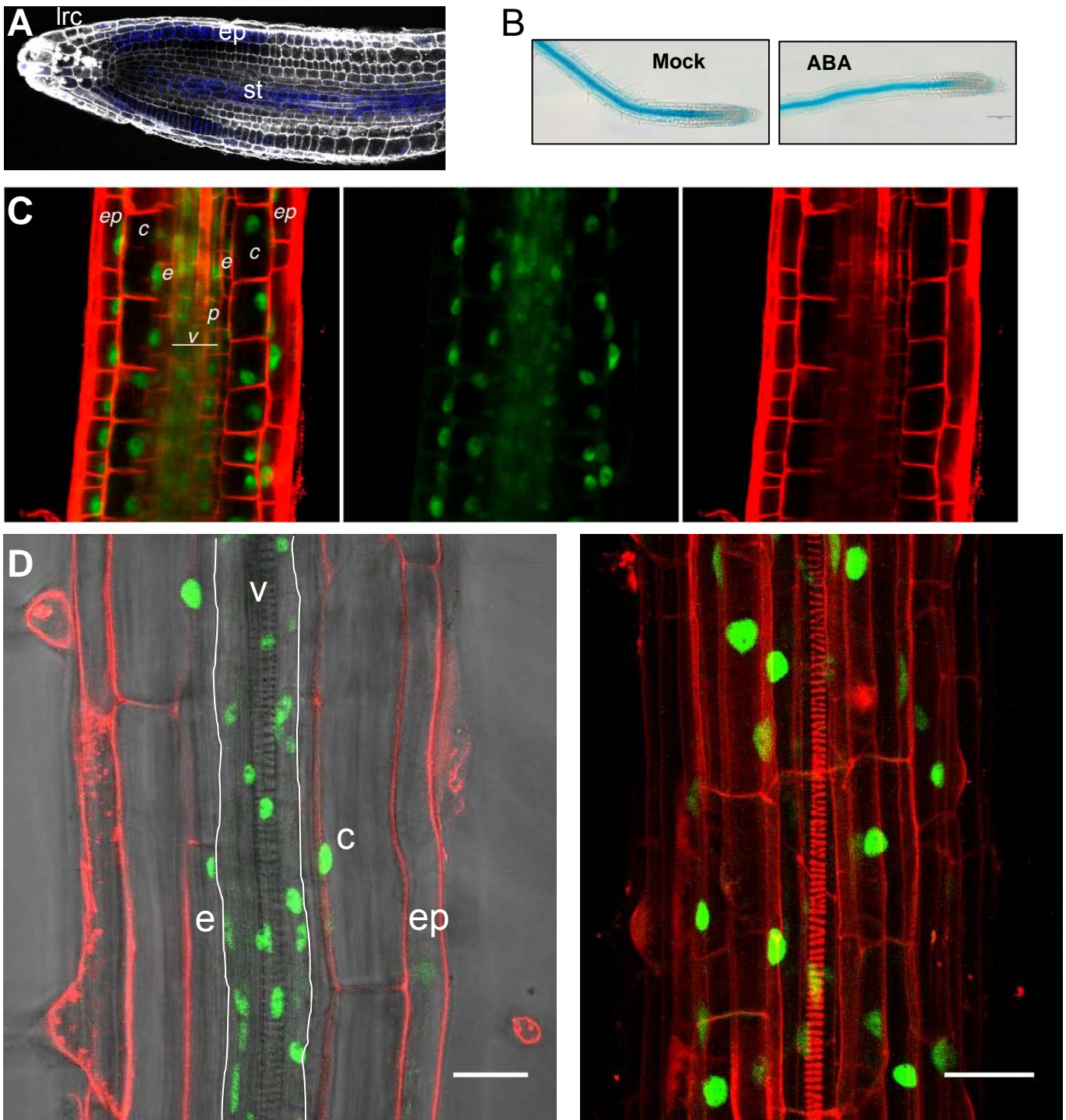


Fig. S5. *ProPYL8:GUS* and *ProPYL8:PYL8-GFP* expression. (A) Expression of *ProPYL8:GUS* in root meristem and elongation zone. GUS expression visualized using modified PS-PI staining and confocal microscopy. (B) GUS expression driven by the *ProPYL8:GUS* gene in the mature and apical root. GUS staining visualized using optical microscopy after mock- or 50 μ M ABA treatment. Scale bars=100 μ m. (C) Expression of PYL8-GFP in the differentiation root zone. Maximum intensity projections of the stacks in the differentiation zone of *ProPYL8:PYL8-GFP pyl8-1* root treated during 6h with 50 μ M ABA and MG132. The images are colored to indicate GFP (green) and propidium iodide (red). (D) Expression of PYL8-GFP in mature root of *ProPYL8:PYL8-GFP pyl8-1* seedlings treated with 50 μ M ABA. Left panel, z-scan; Right panel, 3D reconstruction obtained from a z-series including 56 images. See also Movie S2 showing 3D-reconstruction. SynaptoRed staining of the root is shown in red. Scale bars=30 μ m. Abbreviations: ep, epidermis; c, cortex; e, endodermis; lrc, lateral root cap; p, pericycle; st, stele; v, vascular tissue.

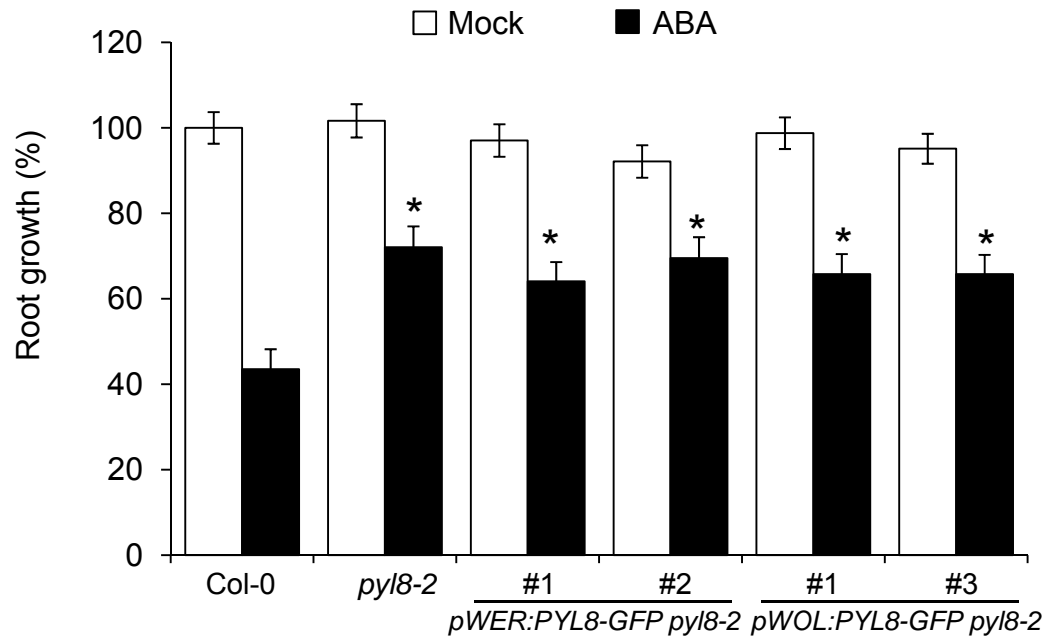


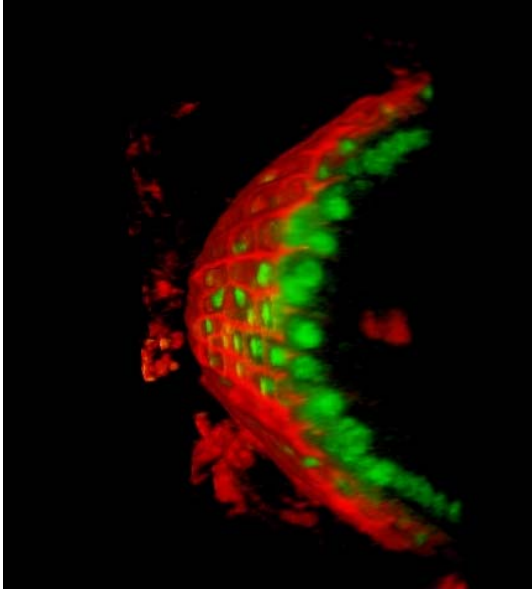
Fig. S6. Lack of complementation of the ABA-insensitive *pyl8-2* phenotype in *pWER:PYL8-GFP* and *pWOL:PYL8-GFP* lines. ABA-mediated inhibition of root growth in the indicated backgrounds. 5-d-old seedlings germinated on MS plates were transferred to new plates lacking or supplemented with 10 μ M ABA and quantification of root growth was performed after 10 d. Data are averages \pm SD from three independent experiments (n=20). * indicates $P < 0.05$ (Student's t test) compared to wild-type Col-0 in the same assay conditions.

SI Table

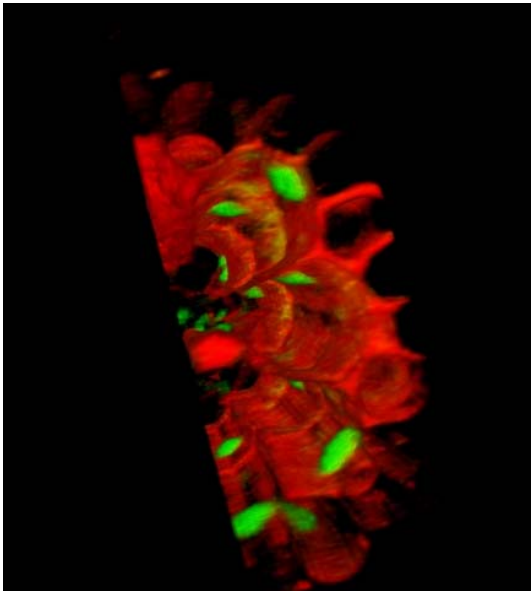
Table S1. List of oligonucleotides used in this work.

ACTGTGAAGCAAACCCCTATA	FpromPYL8
ACCATGGAAGCT AAC GGG ATT GAG	Fpyl8-1NcoI
TTAGACTCTCGATTCTGTCTGT	RvStop PYL8
GACTCTCGATTCTGTCTGTCTGT	RnostopPYL8
AAACTGCAGAAGAAGATGGAAGCTAACGGGATT	FwPstIPYL8
AAAGGATCCTTACTTGTACAACCTCATCCATGCC	RvBamHIGFP
CCACAGAAGTATAGGCCGTTTATCAGT	FK61R PYL8
ACTGATAAACGGCCTATACTTCTGTGG	RK61R PYL8
ATCATCTCTCTTACCCCCGAGACTATA	PYL8Y120A-F3
CTTAAGAACGCTTCTTCAATCATCTCTCTTACCCCCGAGACTATA	PYL8Y120A-FT3
TCTATGATCACCACCAACGATTCTGAT	PYL8Y120A-R3
TGAAGAAGCGTTCTTAAGTCTATGATCACCACCAACGATTCTGAT	PYL8Y120A-RT3
ACCATGGCGAATTCAGAGTCCT	FNco5g46790PYL1
GGATCCTTACCTAACCTGAGAAGAGTTGT	RBamHI5g46790PYL1
ACCATGGGCTCATCCCCGGCCGTGA	FwNcoPYL2
TTATTCATCATCATGCATAGGTG	RvStopPYL2
ACCATGGCAACGTCGATACAGTT	FNcoI2g40330PYL6
TTACGAGAATTTAGAAGTGTT	R2g40330PYL6
ACCATGGAGATGATCGGAGGAGAC	F PYL7
TCAAAGGTTGGTTTCTGTATGATTC	R PYL7
ACC ATG GTG GAC GGC GTT GAA GGC	FwNcoIPYL9
TCA CTG AGT AAT GTC CTG AGA	RvPYL9
ACCATGGACGGTGACGAAACAAAGAAG	F PYL10
TCATATCTTCTTCTCCATAGATTC	R PYL10
TCTTTAGCTGATATCTCTGAACGTC	F507PYL8
AAGAGGGTTTGAAAGTGAAATGACC	R760PYL8
CATAACCCAACGCATCCA	FwPYL2 RT-qPCR
AACTCAAGCCGCTCGGTA	RvPYL2 RT-qPCR
CTCCGGGACCGTCGTTGT	FwPYL4 RT-qPCR
GGGTGGTGAAAGCCGAA	RvPYL4 RT-qPCR
TGTAGCTCTACGCTTGTT	FwPYL8 RT-qPCR
GTTGCTGGTAGTCCAGAT	RvPYL8 RT-qPCR
ACCAGTGTACCTCTGCTC	FwPYL9 RT-qPCR
TCTAAGACTGCCGATTTTC	RvPYL9 RT-qPCR
AGTGGTCGTACAACCGGTATTGT	Fw ACT8 RT-qPCR
GAGGATAGCATGTGGAAGTGAGAA	Rv ACT8 RT-qPCR

SI Movies



Movie S1. Expression of PYL8-GFP in epidermis of the root apex from *ProPYL8:PYL8-GFP pyl8-1* seedlings treated with 10 μ M ABA for 6h. 3D reconstruction obtained from a z-series including 56 images.



Movie S2. Expression of PYL8-GFP in mature root of *ProPYL8:PYL8-GFP pyl8-1* seedlings treated with 50 μ M ABA for 6h. 3D reconstruction obtained from a z-series including 56 images.

SI References

1. Santiago J, et al. (2009) Modulation of drought resistance by the abscisic acid receptor PYL5 through inhibition of clade A PP2Cs. *Plant J* 60: 575-588.
2. Pizzio GA, et al. (2013). The PYL4 A194T mutant uncovers a key role of PYR1-LIKE4/PROTEIN PHOSPHATASE 2CA interaction for abscisic acid signaling and plant drought resistance. *Plant Physiol* 163: 441-455.
3. Bueso E, et al. (2014). The single-subunit RING-type E3 ubiquitin ligase RSL1 targets PYL4 and PYR1 ABA receptors in plasma membrane to modulate abscisic acid signaling. *Plant J* 80: 1057-1071.
4. Belda-Palazon B, et al. (2016) FYVE1/FREE1 Interacts with the PYL4 ABA Receptor and Mediates its Delivery to the Vacuolar Degradation Pathway. *The Plant Cell* 28: 2291-2311.
5. Michniewicz M, Frick EM, Strader LC (2015) Gateway-compatible tissue-specific vectors for plant transformation. *BMC Res Notes* 8: 63.
6. Dietrich D, et al. (2017) Root hydrotropism is controlled via a cortex-specific growth mechanism. *Nat Plants* 3: 17057.
7. Chiu J, March PE, Lee R, Tillett D (2004) Site-directed, Ligase-Independent Mutagenesis (SLIM): a single-tube methodology approaching 100% efficiency in 4 h. *Nucleic Acids Res* 32: e174.
8. Dupeux F, et al. (2011) A thermodynamic switch modulates abscisic acid receptor sensitivity. *EMBO J* 30: 4171-4184.
9. Antoni R, et al. (2013) PYRABACTIN RESISTANCE1-LIKE8 plays an important role for the regulation of abscisic acid signaling in root. *Plant Physiol* 161: 931-941.
10. Ferrandiz C, Liljegren SJ, Yanofsky MF (2000) Negative regulation of the SHATTERPROOF genes by FRUITFULL during Arabidopsis fruit development. *Science* 289: 436-438.
11. Pound MP, French AP, Wells DM, Bennett MJ, Pridmore TP (2012) CellSeT: novel software to extract and analyze structured networks of plant cells from confocal images. *The Plant Cell* 24: 1353-1361.